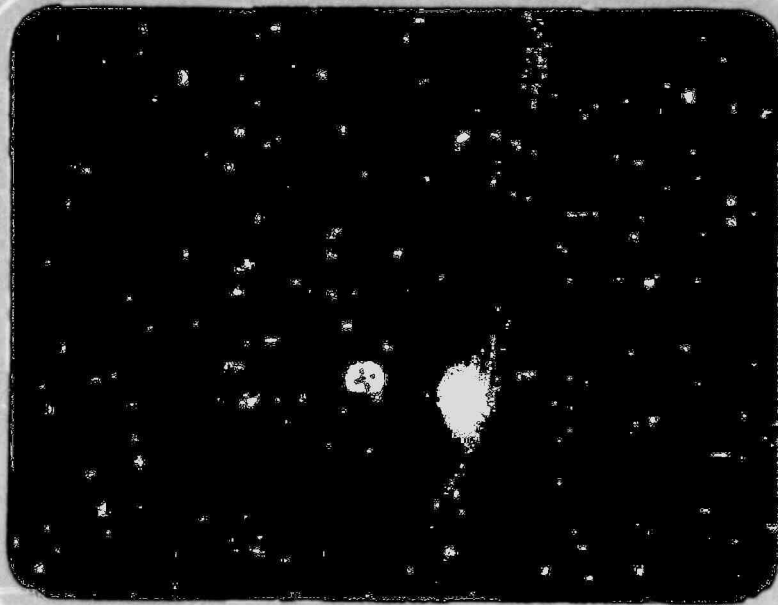




Battelle
Columbus Laboratories

Report



POOR ORIGINAL

2264 200

Exhibit A to Report No. IE-116
by PARAMETER, Inc.
NRC Contract 05-77-186
PAR: NRC-IE-78/79, Task 03

7906210 3391

FINAL REPORT

on

EXAMINATION OF INCONEL
SAFE END FROM DUANE ARNOLD

to

PARAMETER INCORPORATED

January, 1979

by

V. Pasupathi, G.P. Smith, D.R. Farmelo, and J.S. Perrin

2264 201

BATTELLE
Columbus Laboratories
505 King Avenue
Columbus, Ohio 43201

TABLE OF CONTENTS

	<u>Page</u>
INTRODUCTION.1
EXAMINATIONS AND RESULTS.1
Receipt of Shipment.1
Visual Examination1
Dimensional Measurements2
Destructive Examinations2
Tensile Tests.	17
Chemical Analyses.	17
Scanning Electron Microscopy	23
Electron Microprobe (EMP) Analysis of Duane Arnold Sample No. 2.	39
SUMMARY OF OBSERVATIONS AND CONCLUSIONS	39
REFERENCES.	45

2264 202

LIST OF FIGURES

	<u>Page</u>
FIGURE 1. APPEARANCE OF DUANE ARNOLD INCONEL SAFE END IN THE AS-RECEIVED CONDITION.	3
FIGURE 2. LOCATION OF METALLOGRAPHIC AND SEM SPECIMENS ON DUANE ARNOLD SAFE END N2-E	5
FIGURE 3. CONDITION OF SAMPLES AFTER BEING CUT FROM SAFE END.	6
FIGURE 4. CHANGE IN OUTER CIRCUMFERENCE DURING SECTIONING OF DUANE ARNOLD SAFE END	8
FIGURE 5. MICROGRAPH MONTAGE OF CRACK IN SAMPLE 2	10
FIGURE 6. MICROGRAPH MONTAGE OF CRACK IN SAMPLE 4	11
FIGURE 7. TYPICAL MICROSTRUCTURES AT VARIOUS LOCATIONS OF SAMPLE 3 CROSS SECTION	12
FIGURE 8. MICROGRAPH MONTAGE OF CRACK IN SAMPLE 3 AFTER ETCHING	13
FIGURE 9. MICROGRAPH OF AREA A ON FIGURE 8 FROM ETCHED SAMPLE 3	14
FIGURE 10. MICROGRAPHS OF AREAS B AND C FROM FIGURE 8 FROM ETCHED SAMPLE 3	15
FIGURE 11. MICROSTRUCTURE OF THE CRACK INITIATION SITE IN SAMPLE 4.	16
FIGURE 12. APPEARANCE OF THE GREY PHASE ADJACENT TO A TIGHT CRACK BRANCH.	18
FIGURE 13. LOCATION OF THE SECTION FROM WHICH TENSILE TEST SPECIMENS WERE MACHINED.	19
FIGURE 14. SCHEMATIC DIAGRAM INDICATING LOCATION OF TENSILE TEST SPECIMENS MACHINED FROM SAFE END	20
FIGURE 15. TENSILE TEST SPECIMEN DIMENSIONS.	21
FIGURE 16. SEM MICROGRAPH OF GREY PHASE AND CORRESPONDING EDAX ANALYSES OF BASE METAL AND GREY PHASE.	25
FIGURE 17. SEM MICROGRAPH AND CORRESPONDING EDAX ANALYSES FROM SAMPLE 4.	27
FIGURE 18. SEM MICROGRAPH AND CORRESPONDING EDAX ANALYSIS OF IRON RICH MATERIAL IN CREVICE OF SAMPLE 4	28
FIGURE 19. SEM MICROGRAPH AND CORRESPONDING EDAX ANALYSIS OF TITANIUM INCLUSION FROM SAMPLE 4	29
FIGURE 20. SCHEMATIC DIAGRAM OF SAFE END SAMPLE 5 INDICATING FRACTURE SURFACE EXAMINED BY SEM	30
FIGURE 21. PHOTOMACROGRAPH OF FRACTURE SURFACE FROM SAMPLE 5	31

List of Figures (Continued)

	<u>Page</u>
FIGURE 22. SEM MICROGRAPH MONTAGES OF SAMPLE 5 FRACTURE SURFACE.32
FIGURE 23. SEM FRACTOGRAPHS OF SAMPLE 5 NEAR CREVICE33
FIGURE 24. SEM FRACTOGRAPHS OF SAMPLE 5 AT MID FRACTURE.34
FIGURE 25. SEM FRACTOGRAPHS OF SAMPLE 5 AT CRACK TIP35
FIGURE 26. SEM FRACTOGRAPHS OF SAMPLE 5 NEAR CRACK TIP37
FIGURE 27. DUANE ARNOLD SAFE END SULFUR PROFILE ON FRACTURE SAMPLE 1.38
FIGURE 28. SAMPLE 2 MICROPROBE RESULTS42

2264 204

LIST OF TABLES

	<u>Page</u>
TABLE 1. RESULTS OF WALL THICKNESS MEASUREMENTS.	4
TABLE 2. RESULTS OF ROOM TEMPERATURE TENSILE TESTS FOR DUANE ARNOLD INCONEL SAFE END MATERIAL.22
TABLE 3. CHEMICAL ANALYSIS OF INCONEL SAFE END BULK METAL MATERIAL24
TABLE 4. ELECTRON MICROPROBE RESULTS OF 2 θ SCANS IN BASE METAL, GREY PHASE AND WELD METAL40
TABLE 5. ELECTRON MICROPROBE ANALYTICAL RESULTS FOR Ni, Cr, Fe FROM AREA/POINT COUNTING IN BASE METAL, GREY PHASE (POINT), AND WELD METAL41

2264 205

1.0 INTRODUCTION

Recently Iowa Electric Light and Power Company found cracks in all of the eight Inconel safe end sections of the recirculation inlet nozzle in the Duane Arnold Plant. One of the safe ends was found to contain a visible throughwall crack. Cracks in other safe ends were detected by a combination of radiography and ultrasonic techniques. In order to determine the cause(s) of cracking Iowa Electric Light and Power Company initiated examination of the safe end section containing the throughwall crack. In parallel with this effort, examination of another safe end from Duane Arnold was initiated at Battelle's Columbus Laboratories (BCL). This parallel effort had the objective of obtaining an independent evaluation of the nature and extent of cracking.

The safe end designated as N2E was shipped to BCL and subjected to detailed nondestructive and destructive examinations including optical metallography, scanning electron microscopy, electron microprobe analysis, chemical analysis and mechanical property evaluation. This document is a final report of the data obtained in this investigation.

2.0 EXAMINATIONS AND RESULTS

2.1 Receipt of Shipment

The Inconel safe end section was received at the BCL Hot Laboratory during September, 1978. Upon opening the shipping container, the internal activity was found to be rather high, ~500-700 mRem/hr at or near the specimen. In addition the specimen was found to be highly contaminated, with smearable activity being 900,000 dpm.

2.2 Visual Examination

A visual examination of the sample was made using a magnifying glass. Care was taken not to disturb the deposits on the specimen surface. The outer surface of the specimen was relatively clean with azimuthal orientation marks 0-20 around the circumference of the safe end. These markings had been made with a felt tip marker and corresponded to the locations of radiography films.

In addition to these marks, the piece also contained a hose clamp containing the specimen identification number plate showing N2E. The location of the repair weld could be clearly seen on the outer surface. The inner surface of the specimen had a rust colored coating of loose powder. This powder could be easily scraped off. Careful examination of the inner surface failed to reveal any cracks. The as-received condition of the specimen was documented by photography in detail. Figures 1a and 1b show the appearance of the specimen.

2.3 Dimensional Measurements

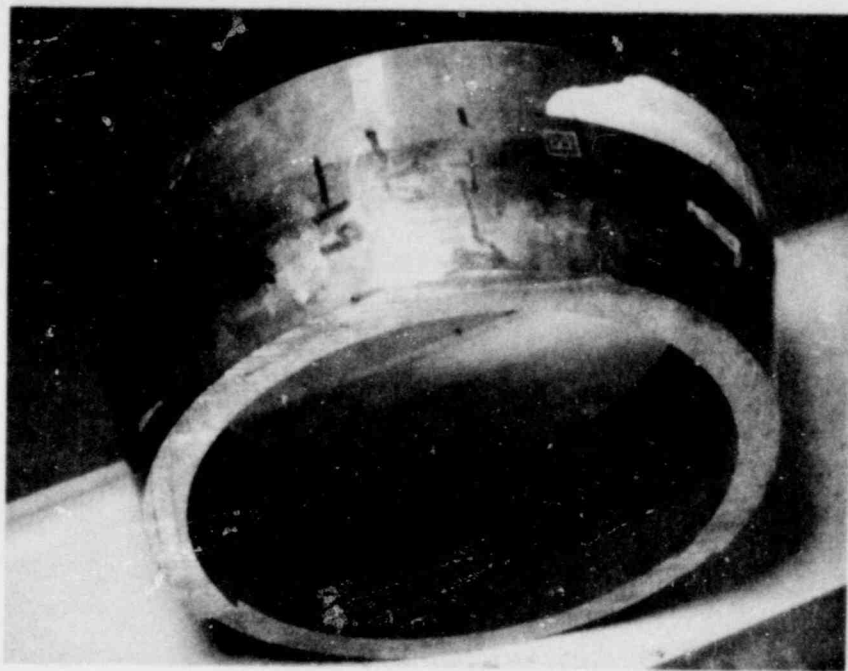
Dimensional measurements made on the specimen consisted of wall thickness and diameter measurements. Wall thickness measurements were made using a micrometer. Location of the measurements and the results are shown in Table 1. Diameter measurements were made from photographs taken during visual examination. The outer diameter at the large end was 14.00 in. and that at the smaller end was 11.3 in.

2.4 Destructive Examinations

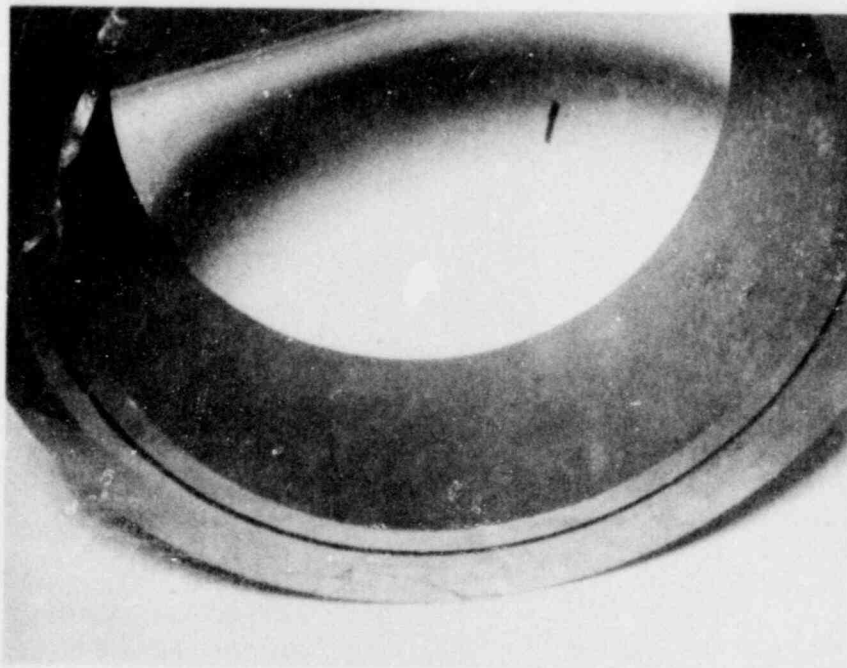
2.4.1 Specimen Sectioning. The specimen was marked for sectioning according to the cutting diagram supplied by Parameter Incorporated. Five thin samples were cut with a band saw. Locations of the samples are shown in Figure 2. Figure 3 shows the samples cut from the safe end.

- Sample No. 1 - At radiography location 5
- Sample No. 2 - Between radiography location 4 and 5
- Sample No. 3 - Between radiography location 3 and 4
- Sample No. 4 - Between radiography location 14 and 15
- Sample No. 5 - Between samples 1 and 2.

2264 207



(a)

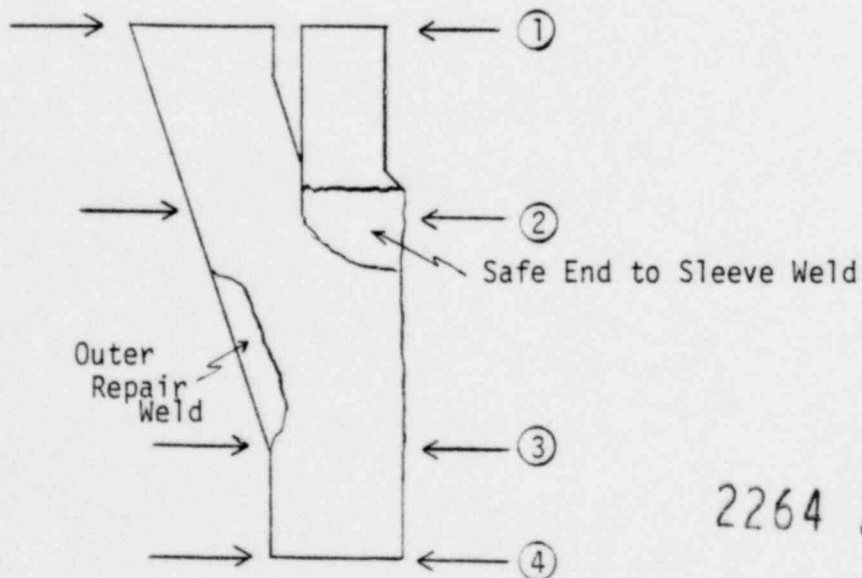


(b)

FIGURE 1. APPEARANCE OF DUANE ARNOLD INCONEL SAFE END IN THE AS-RECEIVED CONDITION

TABLE 1. RESULTS OF WALL THICKNESS MEASUREMENTS

Sector (Orientation)	Locations			
	1	2	3	4
0 (0°)	1.4688"	1.3065"	0.8642"	0.7515"
3 (45°)	1.4850"	1.3030"	0.8610"	0.7450"
5 (90°)	1.4862"	1.2988"	0.8592"	0.7380"
8 (135°)	1.4802"	1.3018"	0.8650"	0.7215"
10 (180°)	1.5112"	1.3015"	0.8565"	0.7142"
13 (225°)	1.4715"	1.3038"	0.8420"	0.7190"
15 (270°)	1.4608"	1.3085"	0.8452"	0.7238"
18 (315°)	1.4565"	1.3090"	0.8650"	0.7322"

SCHEMATIC OF SAFE END CROSS SECTION INDICATING
LOCATIONS OF WALL THICKNESS MEASUREMENTS

2264 209

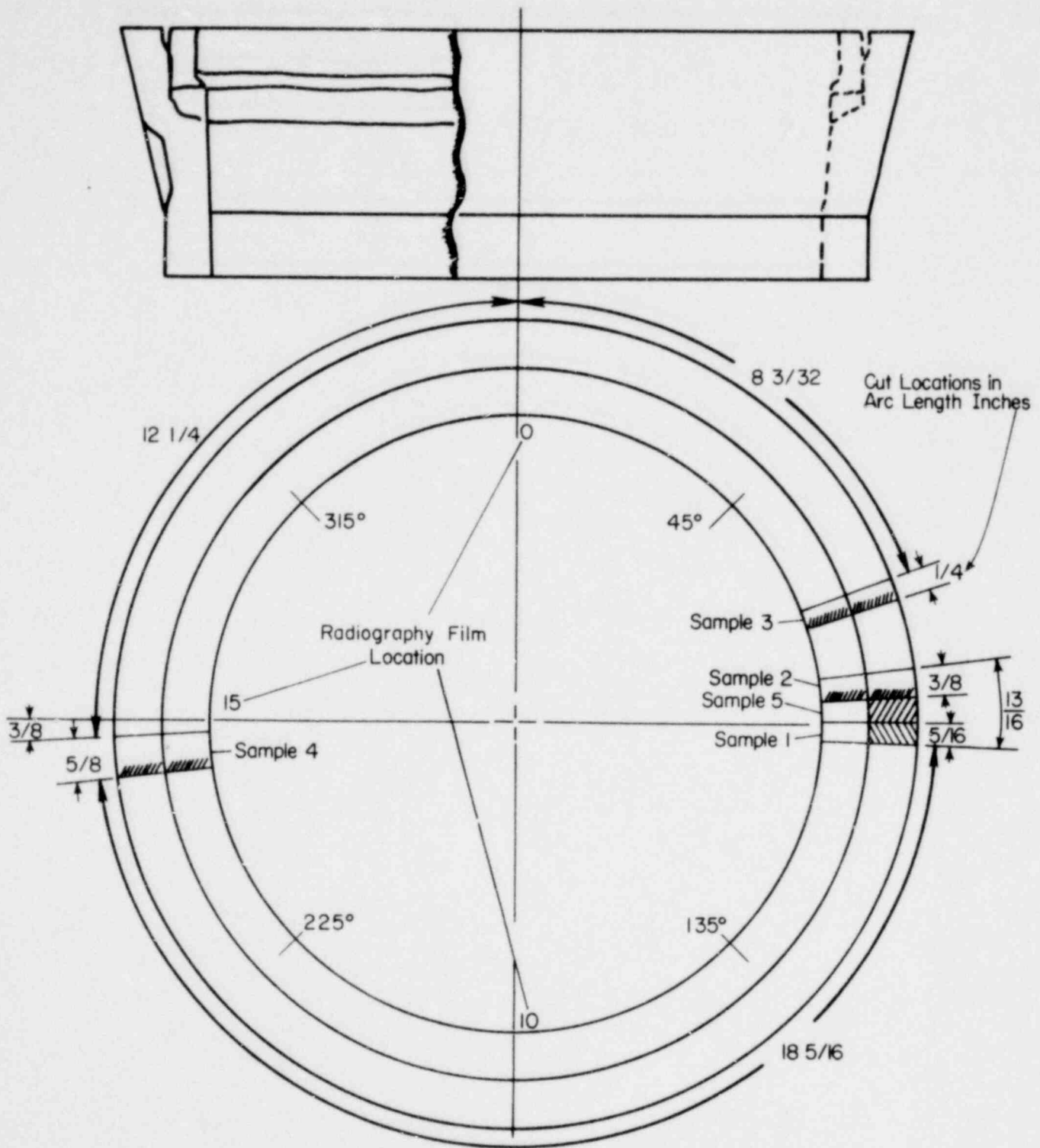
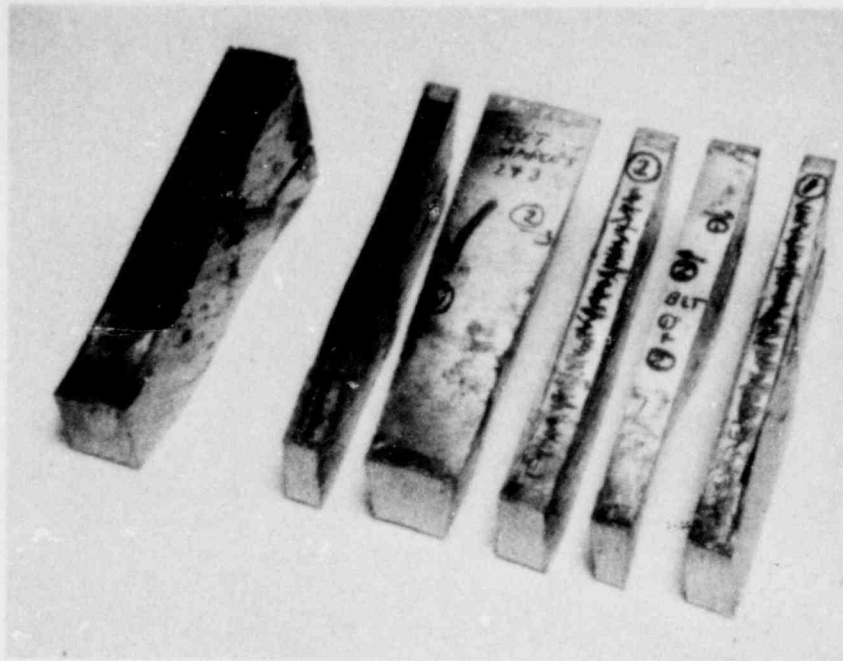
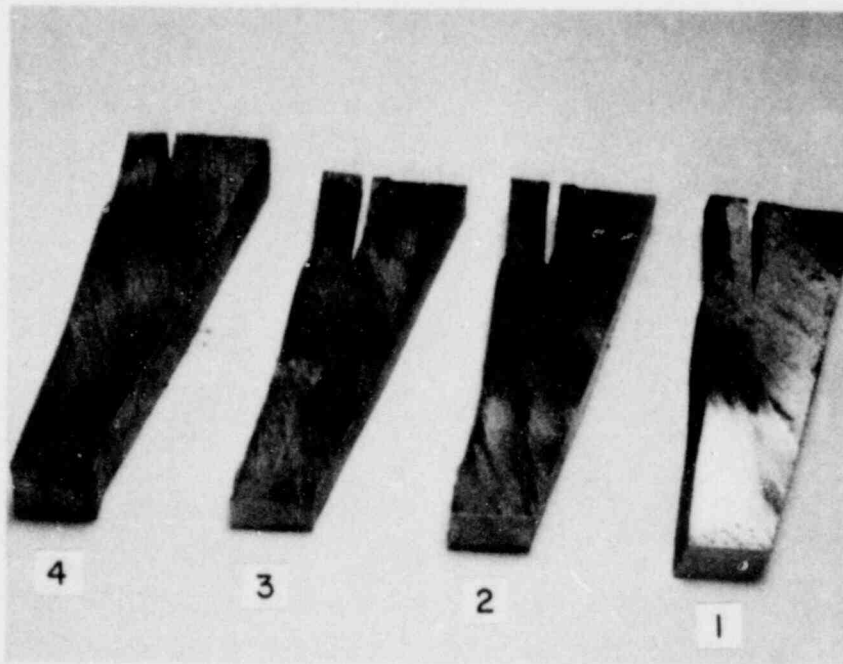


FIGURE 2. LOCATION OF METALLOGRAPHIC AND SEM SPECIMENS ON DUANE ARNOLD SAFE END N2-E



(a)



(b)

FIGURE 3. CONDITION OF SAMPLES AFTER BEING CUT FROM SAFE END

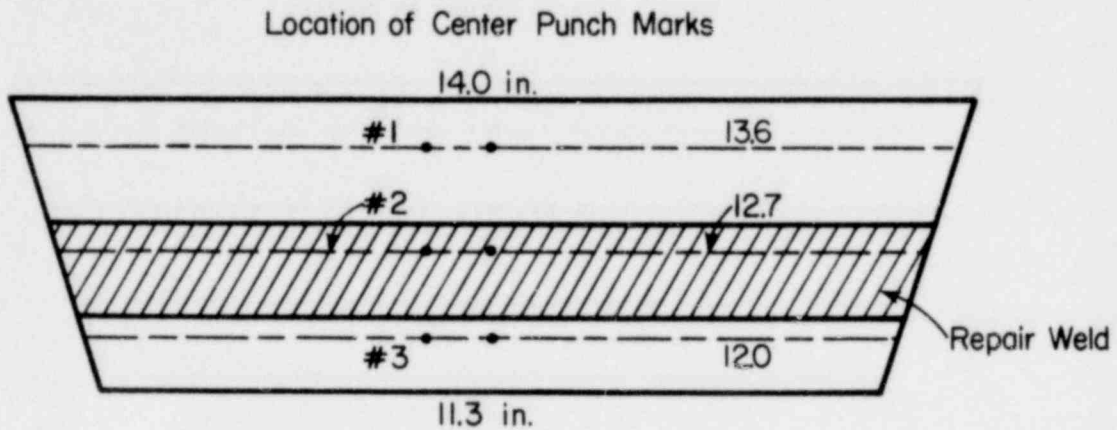
Prior to making the first cut, small indentations were made with a center punch on either side of the first cut location. The distances between these marks were measured. Three such pairs of indentations were made and the distances measured.

While the first cut for Sample No. 1 was being made, it was found that the cut closed tightly and the band saw blade could not be pulled out. The frame was removed and the blade was left in the cut. A new blade was inserted and the second cut made. After completing this cut the sample had to be pried loose. The distance between the centerpunch marks was measured after the sample was cut out. The measurements obtained before and after are shown in Figure 4. Also shown are the locations of the marks.

2.4.2 Metallographic Examination. Samples 2, 3, and 4 were mounted in epoxy resin and prepared for metallographic examination. The samples were milled to obtain a flat surface and ground with silicon carbide papers of grit 120 through 600. They were then polished with a slurry of Linde A alumina. Samples 2 and 4 were examined in the as-polished condition and Sample 3 was etched electrolytically with a 10 percent solution of oxalic acid.

All three samples contained cracks. The cracks were all intergranular in nature. In all samples, the initiation site of cracks was in the region of tight crevice between the sleeve and the safe end and radiated outward. The length of the tight crevice was found to be in the range 0.2-0.3 in. and the width was 0.002-0.005 in. No cracks were observed in the sleeve. In Samples 2 and 4 some grey areas were observed adjacent to tight branches of the cracks. These areas appeared to be of different composition. Similar areas were also observed along "tunnels" radiating from the cracks. The source of this grey phase area is not known.

The crack did not penetrate through the cross section of the safe end in any of the samples examined. In Samples 2 and 3 the crack had penetrated approximately 80% of the wall. In Sample 4, which was obtained



Distance Between Punch Marks Inches

	<u>Before Cut</u>	<u>After Cut</u>	<u>Change</u>
No. 1	0.9230	0.8754	0.0476
No. 2	1.0220	0.9250	0.0970
No. 3	0.9650	0.8800	0.085

FIGURE 4. CHANGE IN OUTER CIRCUMFERENCE DURING SECTIONING OF DUANE ARNOLD SAFE END

2264 213

from the opposite quadrant, the crack penetration was about 30%. The crack characteristics were documented by photography. Figures 5 and 6 show the results from Samples 2 and 4, respectively.

Sample 3 was examined in detail to characterize the microstructure of various parts of the sample. Figure 7 shows the results. The photomicrographs show that no major abnormalities are apparent in the microstructure of the safe end with the exception of sensitization near the sleeve to safe end weld. However, it appears that the thermal sleeve is sensitized (as evident from carbides precipitated at grain boundaries) rather uniformly even away from the weld.

Sample 3 was subsequently reprepared and etched with a mixture of 20 ml H_2O , 20 ml HNO_3 , and 80 ml HCl . The purpose of this procedure was to clearly identify the location of the crack with respect to the weld and heat affected region. With this technique, the crack initiation site was found to be in the re-solution treated region of the heat affected zone. Figures 8 through 10 show details of the crack location and crack characteristics.

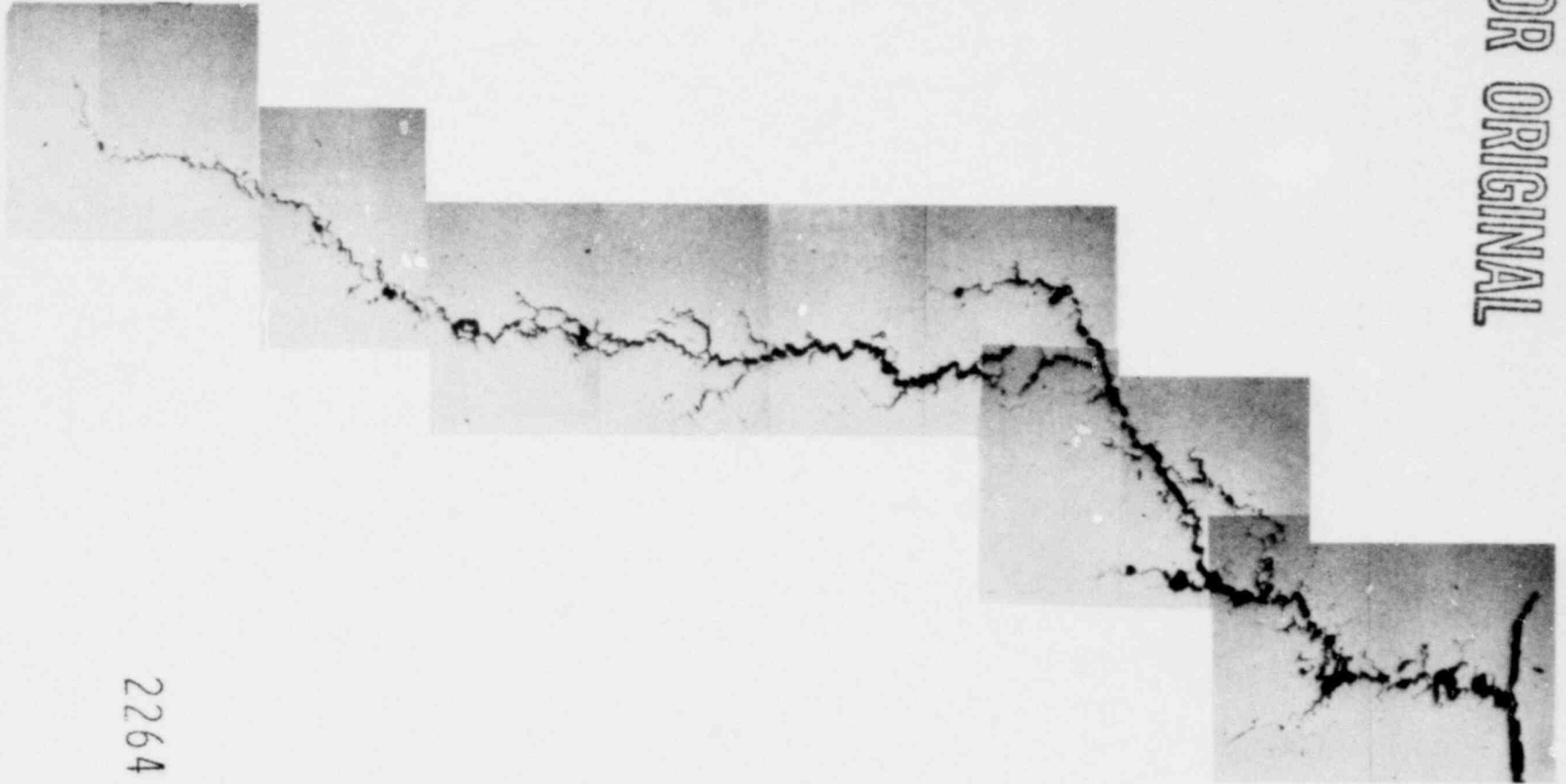
In order to further characterize the extent of sensitization of the safe end in the vicinity of the crack, sample 4 was repolished and electrolytically etched with 10% Nital. This procedure is expected to show grain structure in the material regardless of the degree of sensitization. After examination, the sample was repolished and etched electrolytically with a 15% solution of phosphoric acid. This etching process preferentially attacks carbides in the grain boundaries and the matrix. Figure 11 shows a comparison of the microstructure at the crack initiation site with the two etching procedures. Examination of the photomicrographs shows that the sensitized region in the safe end is rather narrow and that the crack initiation site is located in the re-solution treated region adjacent to the weld. The thermal sleeve also appears to be sensitized to a greater extent in comparison to the safe end.

Additional experiments were carried out on sample 4 using modified glyceresia as the etchant. The etching solution consisted of 10 ml HNO_3 , 10 ml acetic acid, 20 ml HCl and 30 ml glycerine. This process was expected to delineate chromium depleted regions along grain boundaries.⁽¹⁾

(1) References at end of text.

POOR ORIGINAL

10



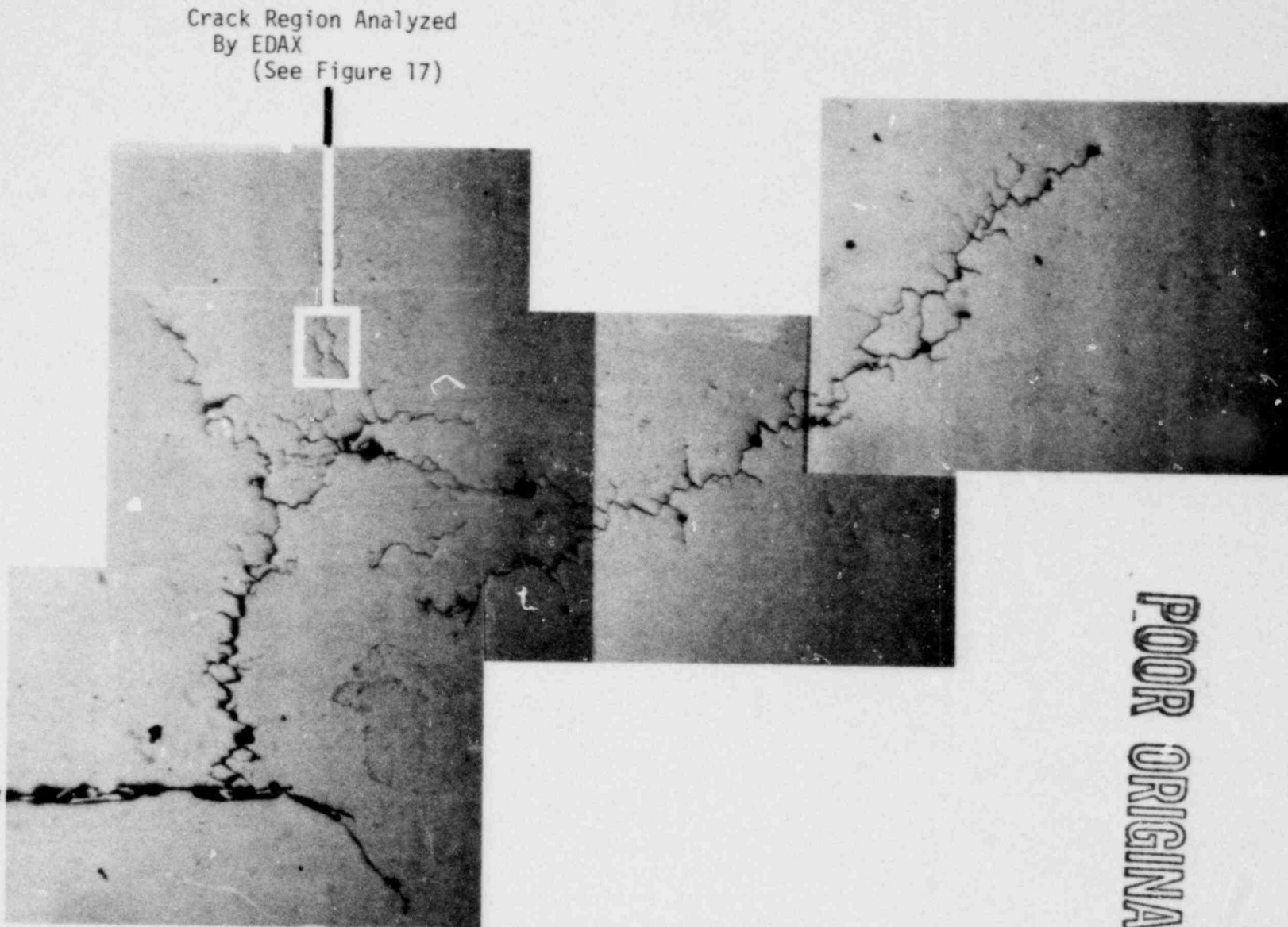
Crevice

FIGURE 5. MICROGRAPH MONTAGE OF CRACK IN SAMPLE 2

2264 215

2264 216

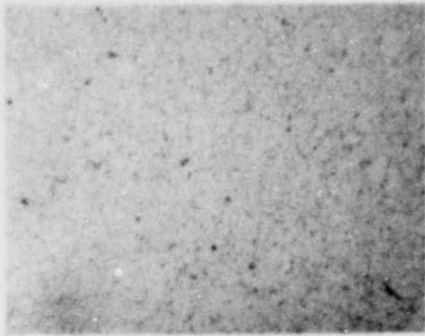
Crevice



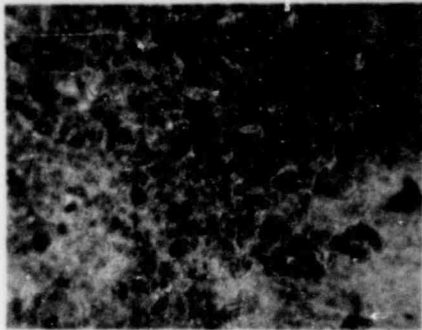
POOR ORIGINAL

FIGURE 6. MICROGRAPH MONTAGE OF CRACK IN SAMPLE 4

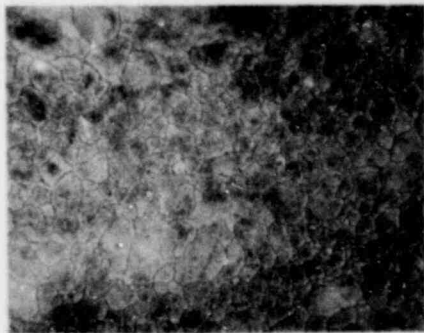
POOR ORIGINAL



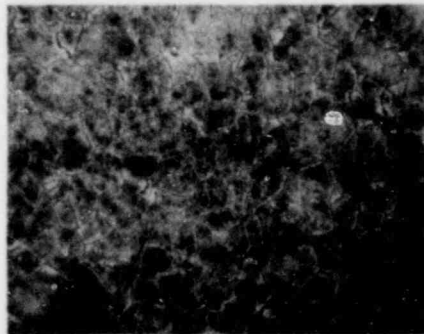
Area 10



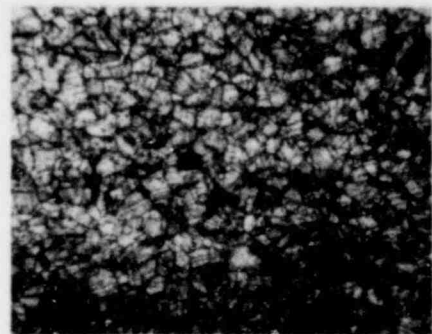
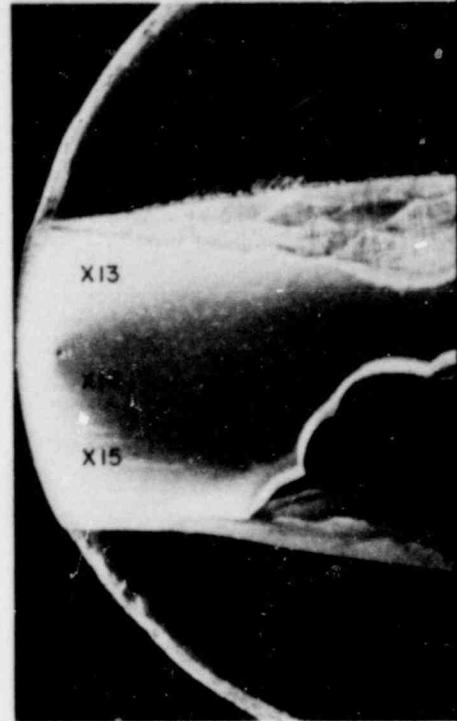
Area 12



Area 13



Area 15

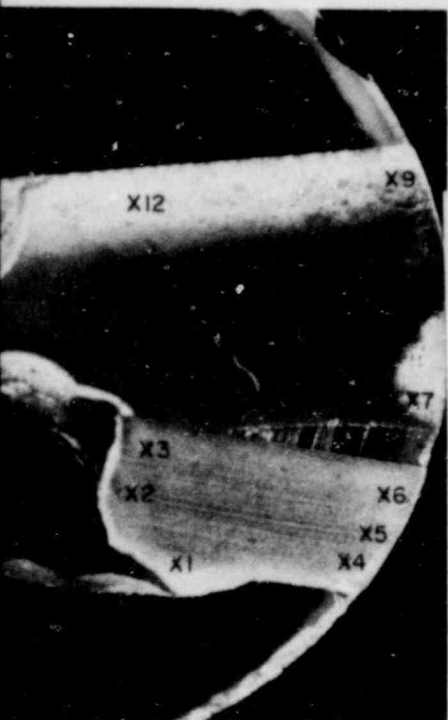


Area 1

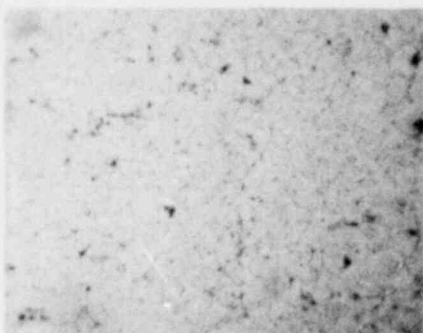
FIGURE 7. TYPICAL MICROSTRUCTURES AT VARIOUS LOCATIONS OF SAMPLE 3 CROSS SECTION

2264 217

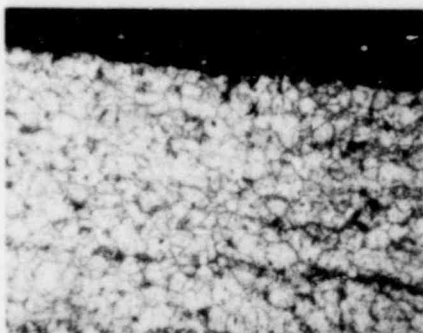
POOR ORIGINAL



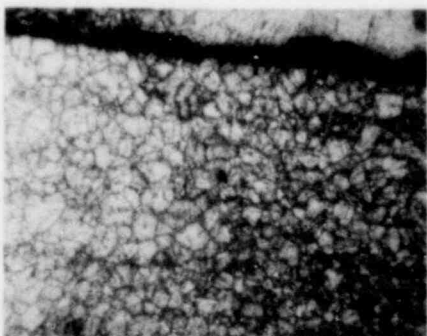
Area 9



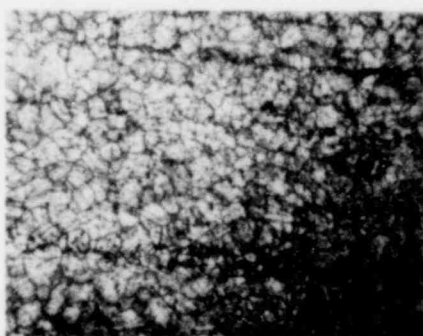
Area 7



Area 6



Area 3



Area 4

2264 218

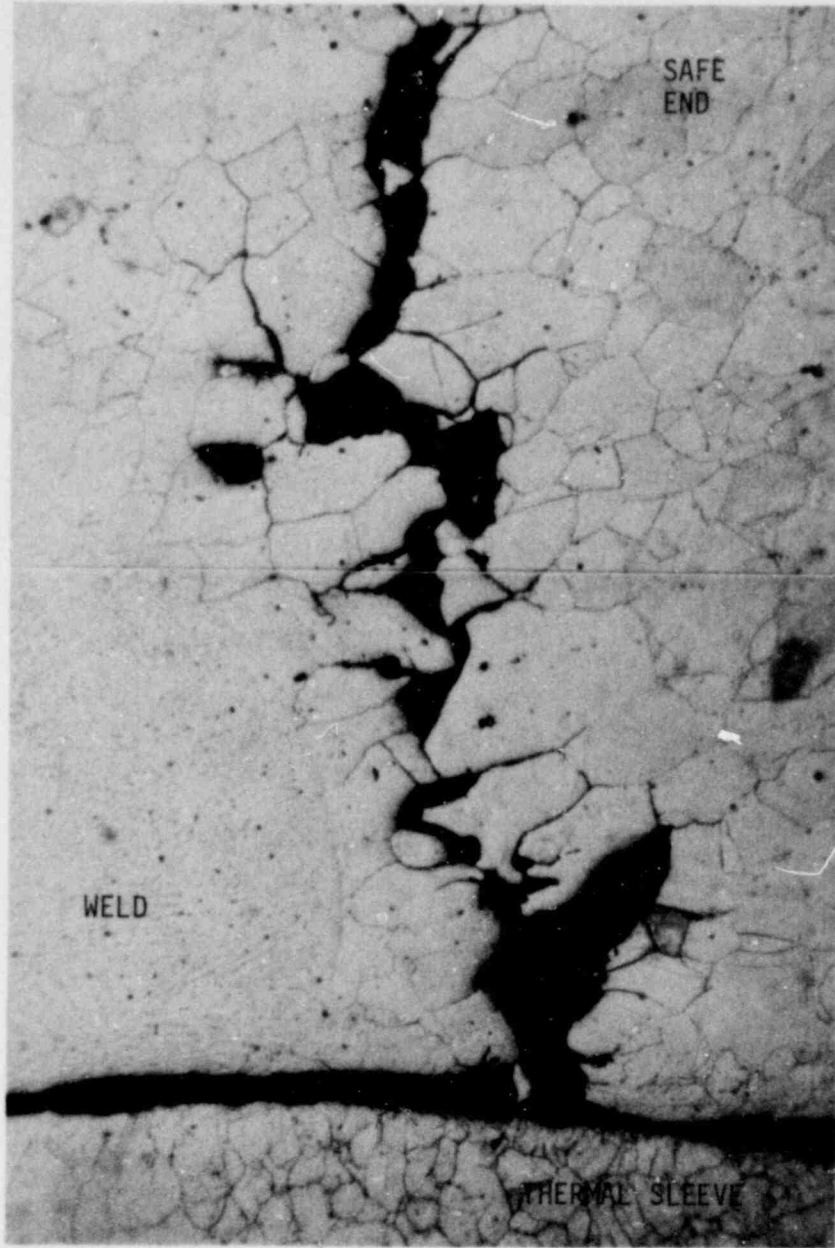


FIGURE 8. MICROGRAPH MONTAGE OF CRACK IN SAMPLE 3 AFTER ETCHING
Details of areas labeled A, B, and C are presented at
higher magnification in Figures 9 and 10.

2264 .219

POOR ORIGINAL

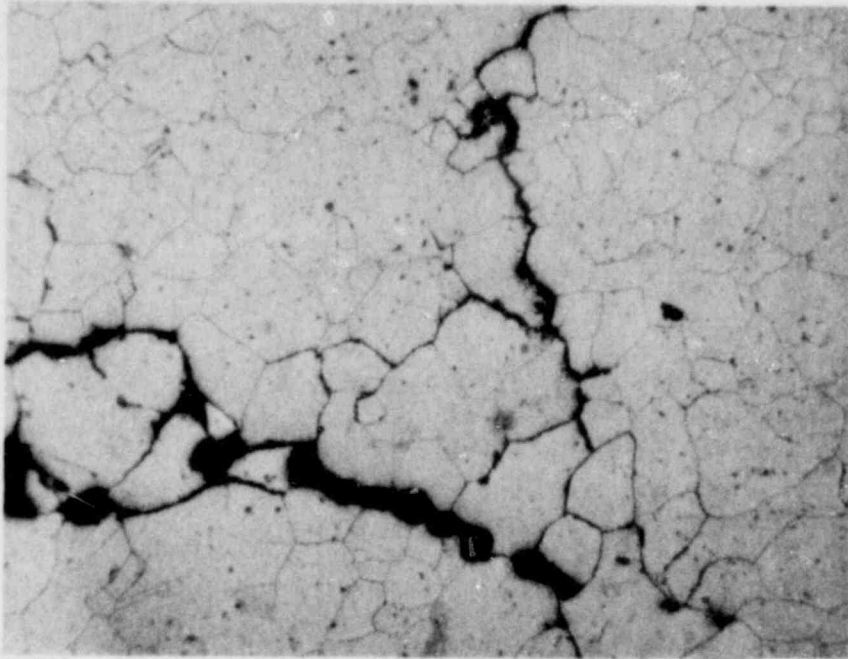
POOR ORIGINAL



100X

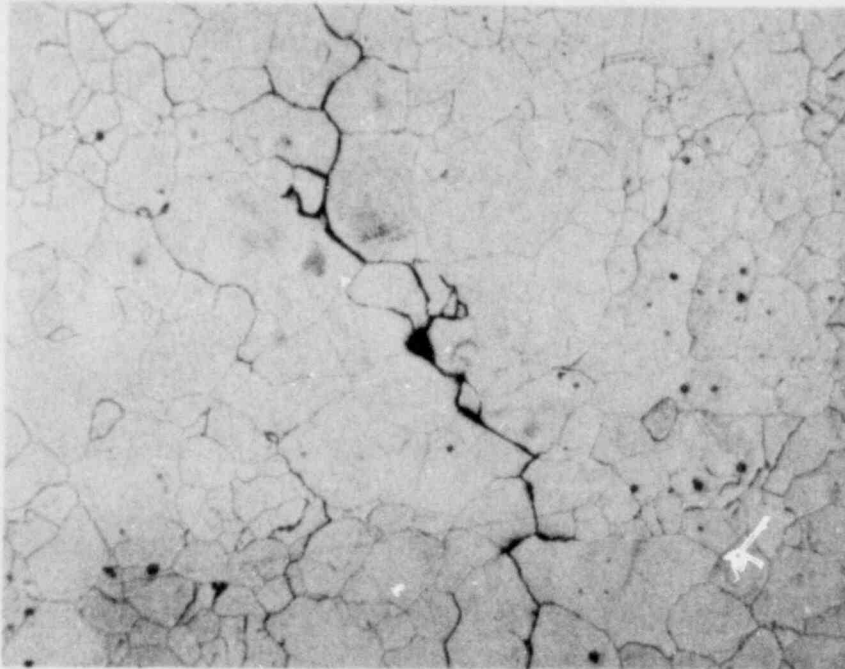
FIGURE 9. MICROGRAPH OF AREA A ON FIGURE 8 FROM ETCHED SAMPLE 3

2264 220

POOR ORIGINAL

100X

(B)



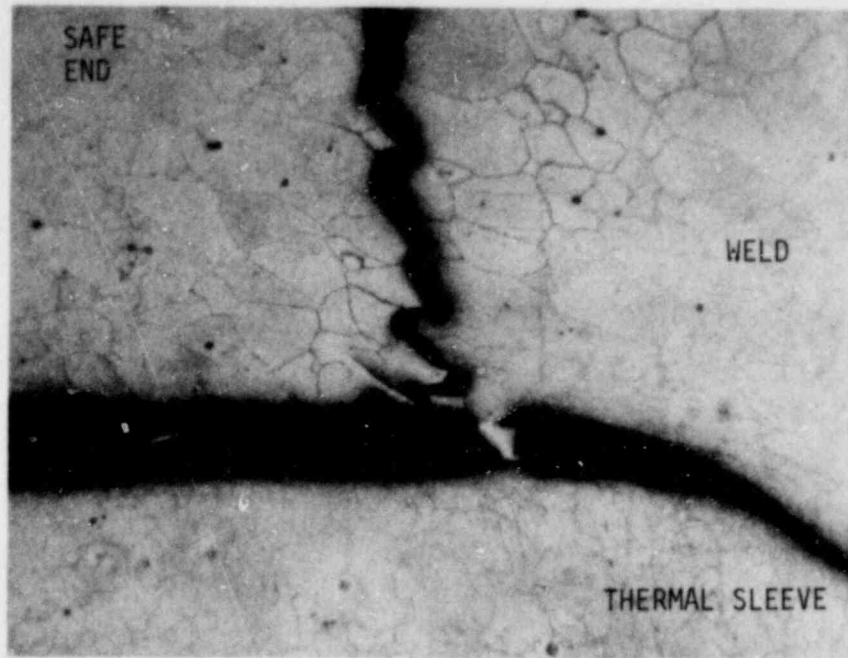
100X

(C)

FIGURE 10. MICROGRAPHS OF AREAS B AND C FROM FIGURE 8 FROM ETCHED SAMPLE 3

2264 221

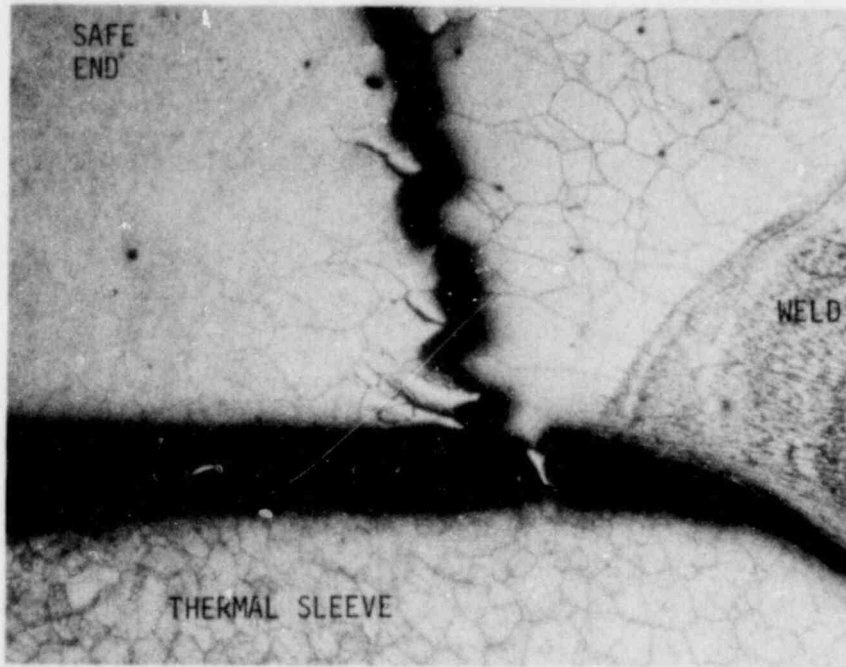
POOR ORIGINAL



100X

19% Nital Etch

(a)



100X

Phosphoric Acid Etch

(b)

FIGURE 11. MICROSTRUCTURE OF THE CRACK INITIATION SITE IN SAMPLE 4

Examination of the specimens showed extremely narrow and barely discernible regions (probably chromium depleted areas) in the relief adjacent to the grain boundaries in the heat affected region. Initially, it was planned to analyze this region using the scanning electron microscope to determine if the composition was different from the grain matrix. This plan was abandoned because of the difficulty in discerning these regions. The etching procedure, however, was found to define more clearly areas previously identified as grey phase. Figure 12 shows one such area in the sample.

2.5 Tensile Tests

From the remaining parts of the Inconel safe end a large piece was sectioned so that specimens for tensile tests could be machined. The large piece was cut between radiography locations 0 and 4 as shown in Figure 13. The cut piece was decontaminated and ultrasonically cleaned and five tensile test specimens were machined. Figure 14 shows schematically the location of the specimens in the safe end and Figure 15 shows the dimensions of the tensile specimens used.

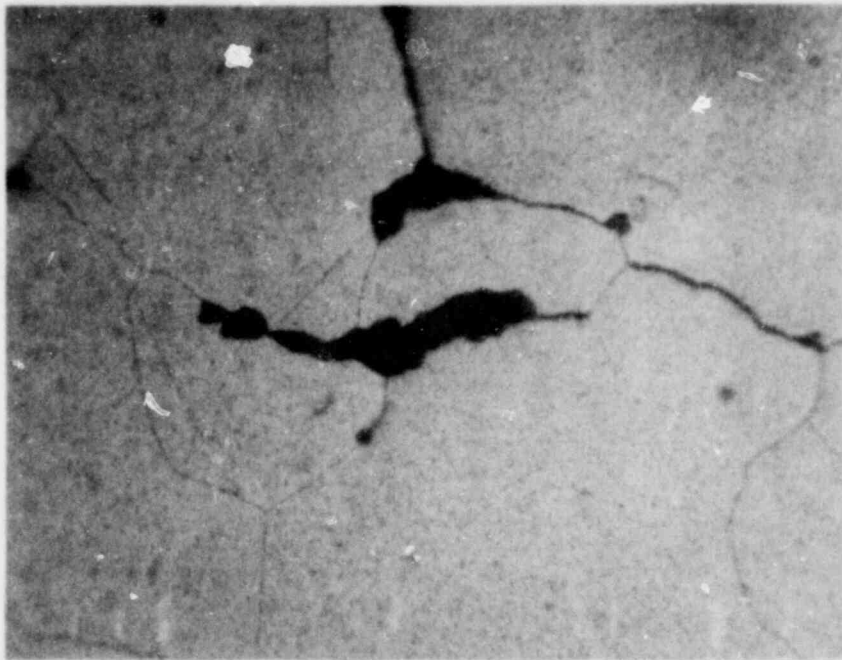
The specimens were tested at room temperature. The results obtained are shown in Table 2. From the results presented in Table 2, it is clear that no degradation of the Inconel safe end tensile properties was observed.

2.6 Chemical Analyses

2.6.1 Tests of pH in Crevice. Tests to determine the pH of the residue in the crevice were carried out using deionized water and litmus paper. Although litmus changes indicated pH to be in the 4-6 range, such reactions were variable and not sufficiently positive to enable conclusive determination of the acidity of corrosion products.

2.6.2 Liquid Samples From Crevice. The section cut from the pipe for tensile test samples was used to obtain samples for chemical analysis. Prior to decontamination the crevice area was rinsed with distilled water and the rinse solution was collected and analyzed by emission spectroscopy. This procedure involves evaporating the water and analyzing the residue. The major element in the residue was found to be Na. Trace amounts of Mn, Si, Cu, Ni, Cr, Ti, Al, B, Fe, Mg, K, Ca, Ba, and Sr were also detected.

POOR ORIGINAL



500X

FIGURE 12. APPEARANCE OF THE GREY PHASE ADJACENT TO A TIGHT CRACK BRANCH

Sample was etched with aqua regia glycerine and acetic acid mixture to reveal chromium depleted regions.

2264 224

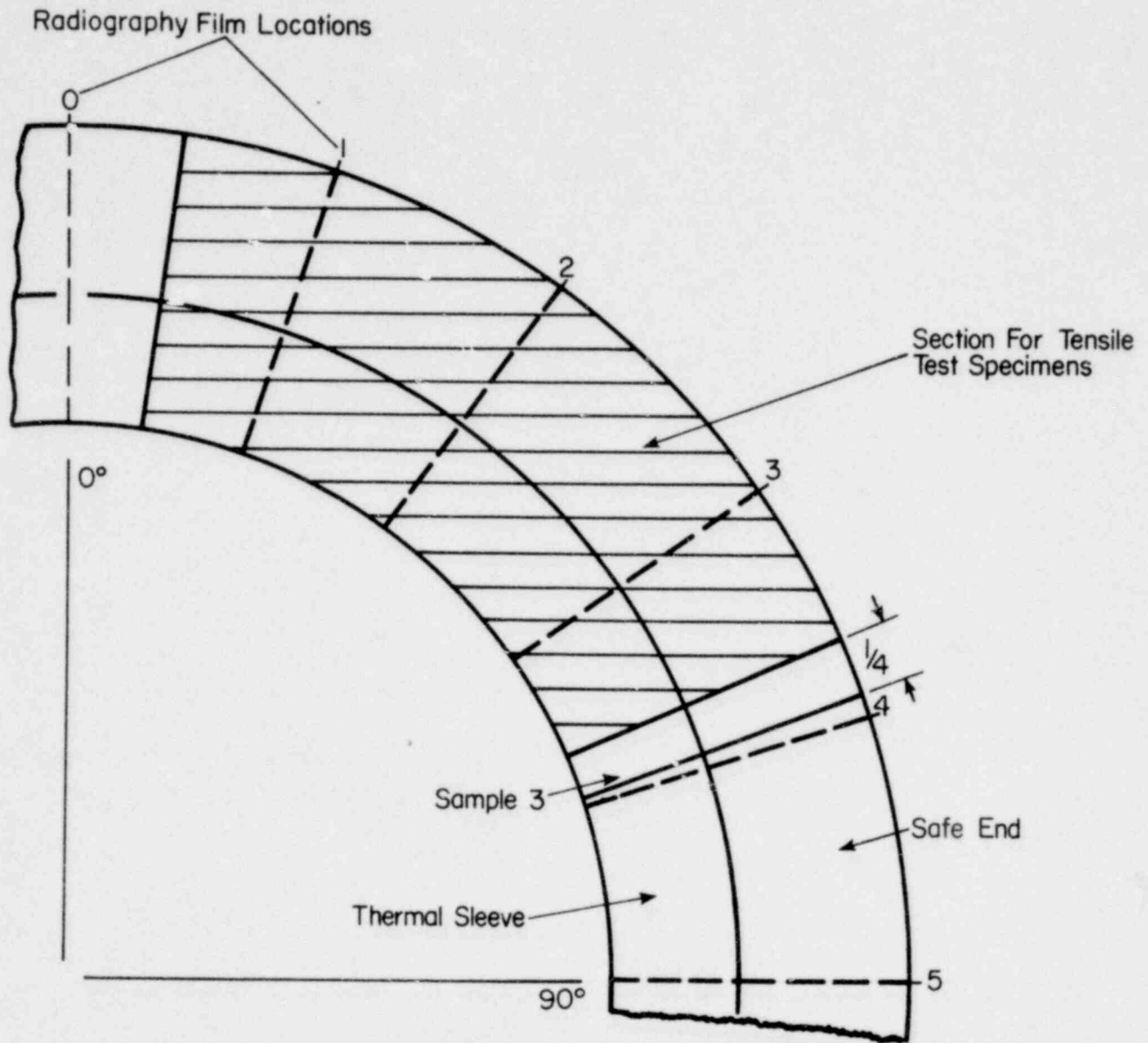
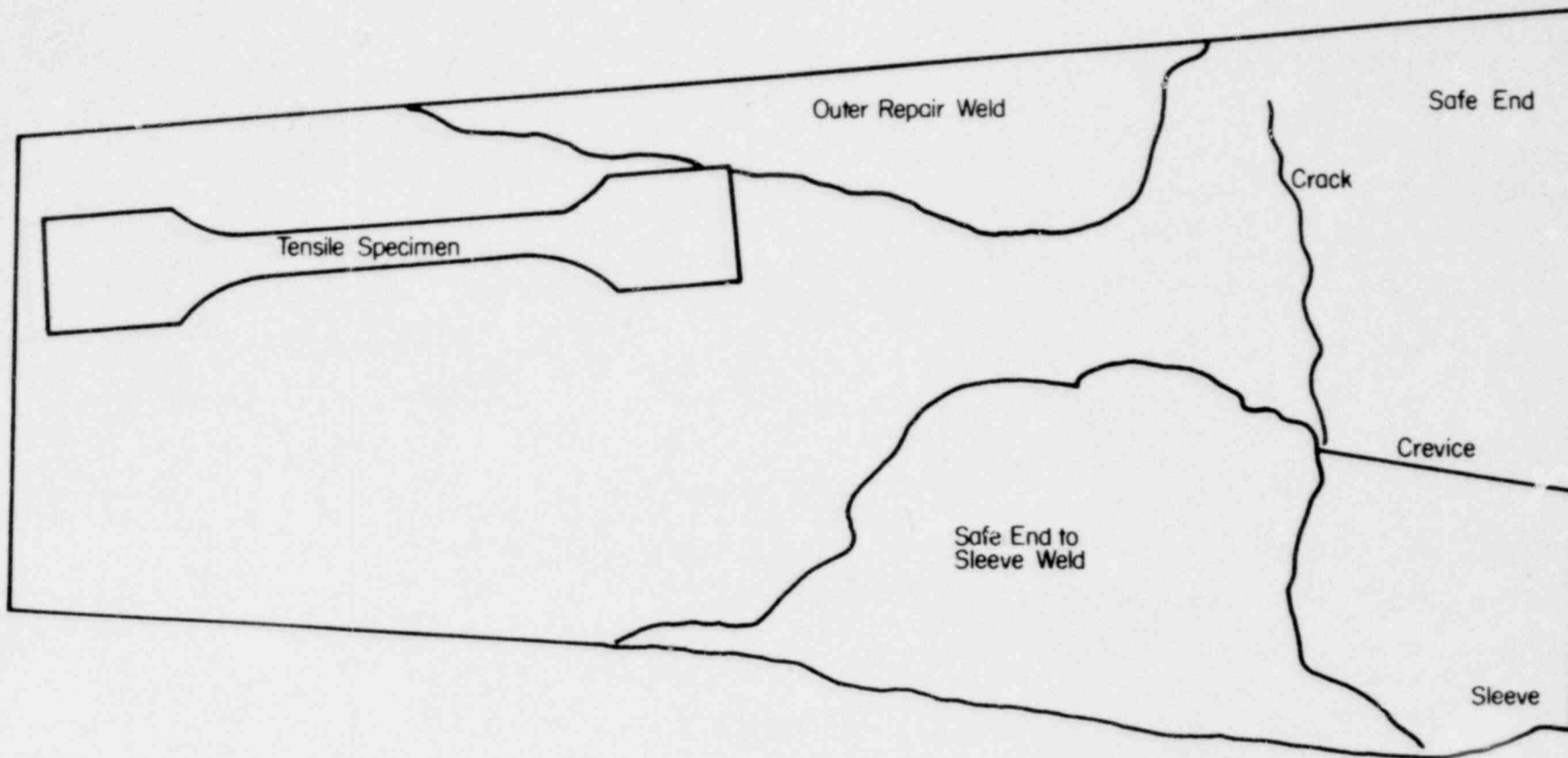


FIGURE 13. LOCATION OF THE SECTION FROM WHICH TENSILE TEST SPECIMENS WERE MACHINED

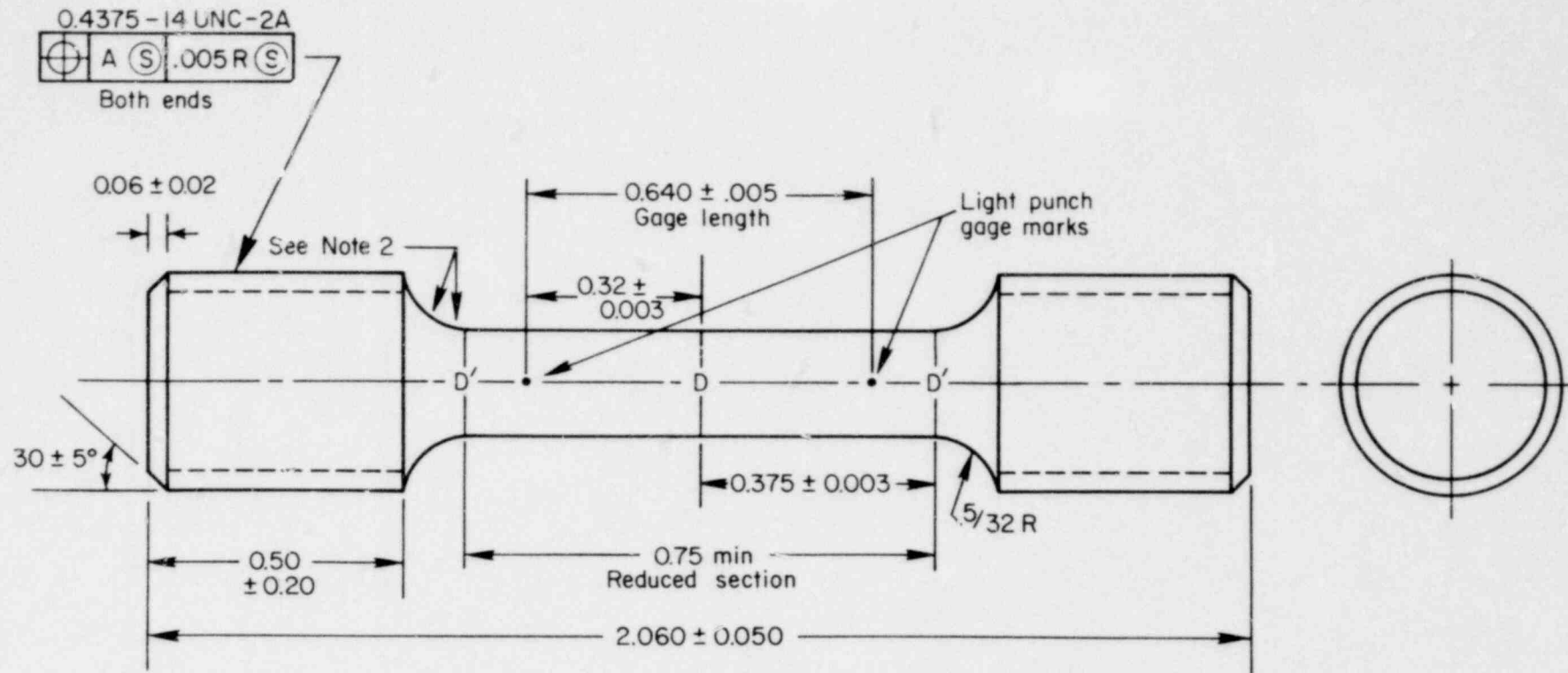
2264 225



20

FIGURE 14. SCHEMATIC DIAGRAM INDICATING LOCATION OF TENSILE TEST SPECIMENS MACHINED FROM SAFE END

2264 226



- Notes: 1. $D = 0.160 \pm 0.001$ diameter at center of reduced section. $D' = \text{actual } D + 0.002 \text{ to } 0.003$ at ends of reduced section tapering to D at center.
2. Grind reduced section and radii to $32\sqrt{\text{radii}}$ to be tangent to reduced section with no circular tool marks at point of tangency or within reduced section. Point of tangency shall not lie within reduced section.

FIGURE 15. TENSILE TEST SPECIMEN DIMENSIONS

2264 227

TABLE 2. RESULTS OF ROOM TEMPERATURE TENSILE TESTS FOR
DUANE ARNOLD INCONEL SAFE END MATERIAL

Test Specimen No.	Yield Strength (ksi)	UTS (ksi)	Percent Total Elongation (in 0.640 in.)	Percent Reduction in Area
DA-1	47.5	107.0	41.9	57.8
DA-2	48.0	106.0	40.15	57.5
DA-3	46.8	105.7	39.5	58.2
DA-4	48.8	104.5	38.3	61.0
DA-5	49.3	107.0	40.6	58.7
Precharacterized* Material	44.0	100.0	38.0	53.0

*Results of Precharacterized Testing obtained from Chicago Bridge and Iron Company Nozzle Certified Test Reports. Specimen gage length for Precharacterized Testing - 2.0 in.

2.6.3 Corrosion Deposits on the Inner Surface of Specimens. The red powdery deposit observed on the inner surface was scraped off and collected. This sample was analyzed using an X-ray diffraction technique. The major portion of the scrapings (60-70%) was found to be hematite (Fe_2O_3). The remainder could not be identified.

2.6.4 Bulk Metal Analysis. Chemical analysis of a bulk metal sample (from safe end) was carried out. The samples consisted of a metal chunk and fine chips. The results, shown in Table 3, indicate that the composition of the material was within the limits of specification.

2.7 Scanning Electron Microscopy

Four safe end specimens, each containing a partial thruwall crack, were examined by scanning electron microscopy (SEM). Two samples (Sample Nos. 2 and 4) were mounted and metallographically polished prior to SEM examination as stated in Section 2.4.2. The remaining SEM samples, identified as Sample Nos. 1 and 5 were examined along the fracture surface. Figure 2 identifies the location and the surfaces examined of each safe end sample.

2.7.1 Polished Samples, SEM Examinations. SEM examination and Energy Dispersive X-Ray Analysis (EDAX) of the fractures and fracture areas of Samples 2 and 4 provided several interesting results. As can be seen from Figures 5 and 6, the cracks observed in both samples contain numerous branches or tributaries. In addition, the cracks appear to originate in the weld heat affected zone at the crevice between the safe end and the thermal sleeve.

SEM examination of many of the tight crack tributaries in Samples 2 and 4 indicated that a phase different from the Inconel base metal was present directly adjacent to the crack. A typical SEM micrograph of this phase with its corresponding X-ray spectrum is presented in Figure 16. EDAX analysis indicated that this grey phase was chromium rich. The chromium enhancement of the grey phase was determined to be approximately 60-80% relative to the base metal material. In addition to the composition variation of the grey phase, numerous instances, of what appears to be transgranular tunneling (shown in Figure 16) were observed in areas where grey phase was found.

TABLE 3. CHEMICAL ANALYSIS OF INCONEL SAFE END
BULK METAL MATERIAL

Element	Percent
Ni	73.6
Cr	15.6
Fe	7.8
Al	0.4
Ti	0.3
Mn	0.2
Si	0.2
Cu	0.1
Mo	0.1
S	0.002
Si	0.3
P	0.03

2264 230

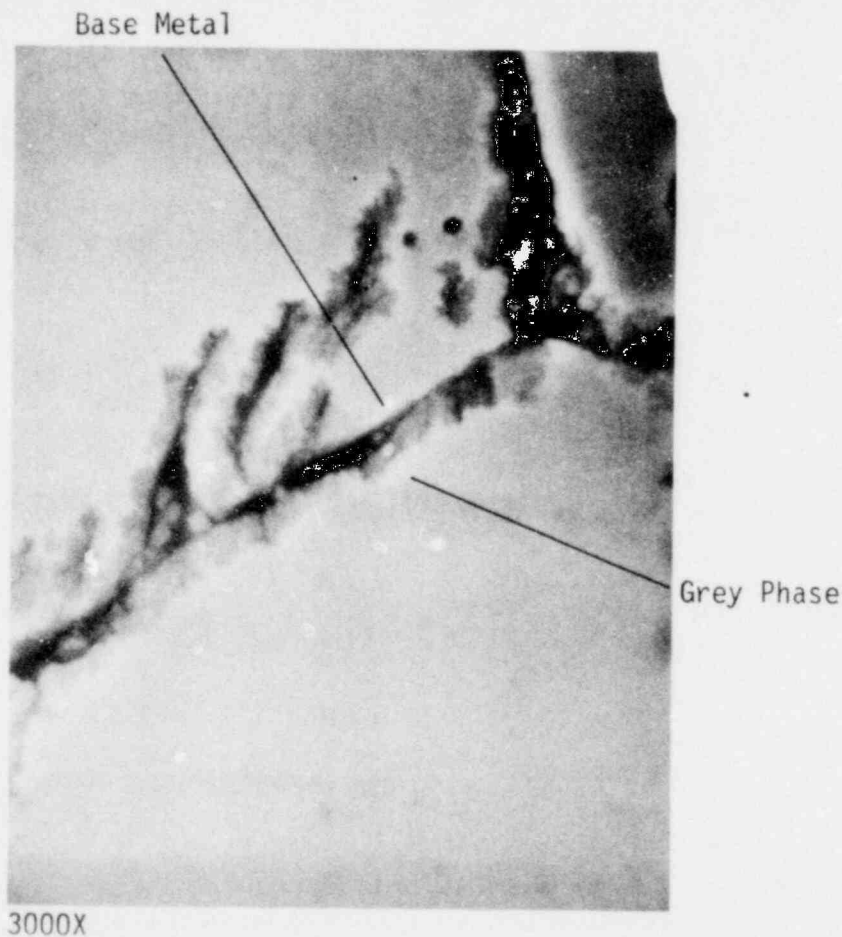
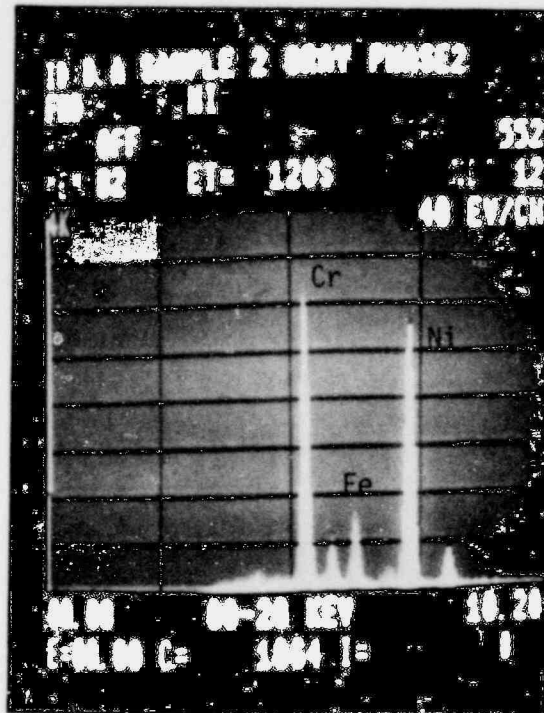
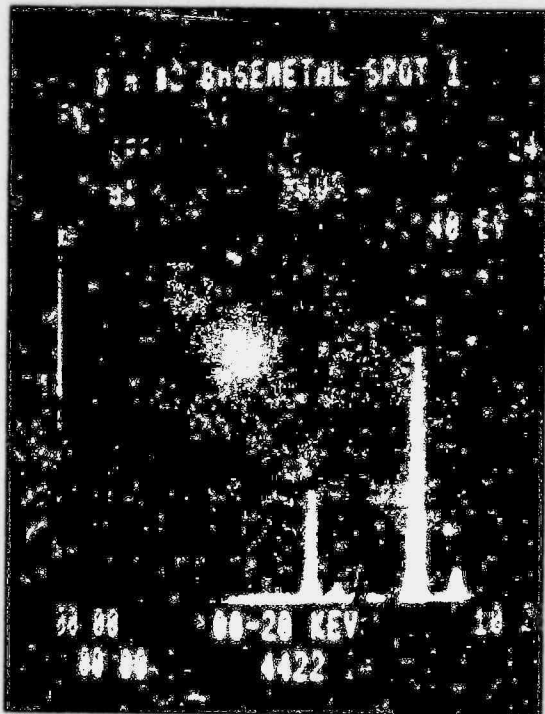


FIGURE 16. SEM MICROGRAPH OF GREY PHASE AND CORRESPONDING EDAX ANALYSES OF BASE METAL AND GREY PHASE

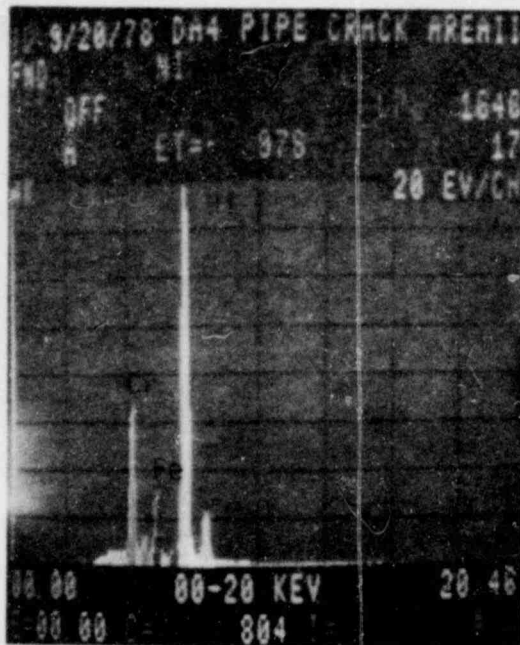
EDAX analysis of material observed within the crack both adjacent to the grey phase and in areas where no grey phase is found indicate an iron rich material relative to base metal compositions. Figures 17 and 18 present SEM micrographs and EDAX spot analysis performed well within the crack and at the crevice on Sample No. 4. As can be seen in Figure 17 the EDAX analysis of material within the crack indicates excessive iron relative to base metal analysis. However, no iron depletion can be observed in the material adjacent to the crack. EDAX analysis performed on material within the crevice (Figure 18) at a location near the crack origin indicate similar iron rich material. Comparison of the two relative iron contents from EDAX analysis at the crevice with analysis in the crack indicate a significantly higher iron content of material well within the crack.

Numerous titanium inclusions were observed throughout the base metal on Samples 2 and 4. A typical titanium inclusion observed in Sample 4 is illustrated by SEM micrograph in Figure 19 in conjunction with its X-ray spectrum.

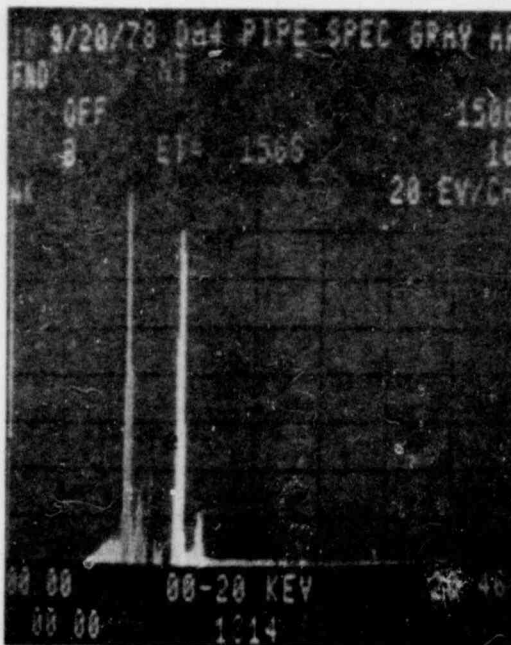
2.7.2 SEM Fractography. As stated previously, safe end Sample No. 5 was examined by SEM. Figure 20 presents a schematic of Sample No. 5 showing the fracture surface examined. In order to expose the fracture surface for examination the specimen was mechanically fractured. Figure 21 presents a photomicrograph of the fracture surface examined. The bright material to the left is the region of uncracked safe end wall thickness which was mechanically fractured. Examination of this region following fracture indicated the material to be ductile.

Detailed SEM examination was performed on the entire fracture surface. Figure 22 presents SEM fractograph montages at the beginning (near crevice) middle, and tip of the crack along the fracture surface. The mode of cracking, as indicated by the SEM fractographs, was intergranular fracture.

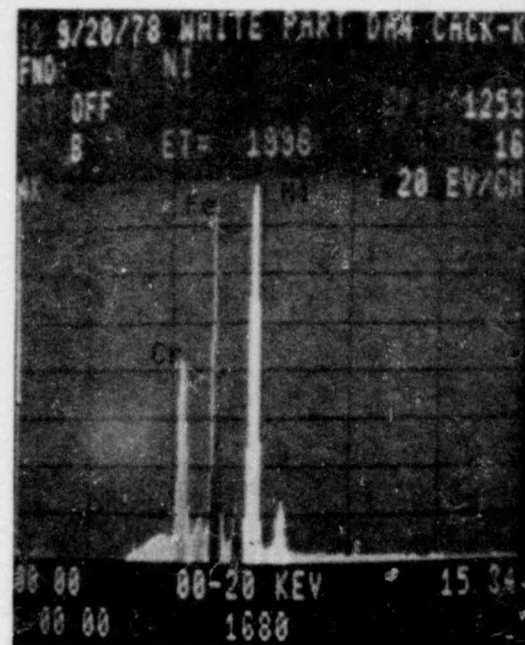
Numerous EDAX analyses were performed on several areas of the fracture and crevice. Figures 23, 24, and 25 present SEM fractographs illustrating typical areas chosen for EDAX analysis (i.e., Figures 23b, 24a, and 25b present actual areas examined by X-ray near the crevice, in the middle and at the tip of the fracture, respectively). In addition, Figure 24b presents a SEM micrograph of a grain facet (from Figure 24a) showing a network of needle-like corrosion products on which a spot EDAX analysis was performed.



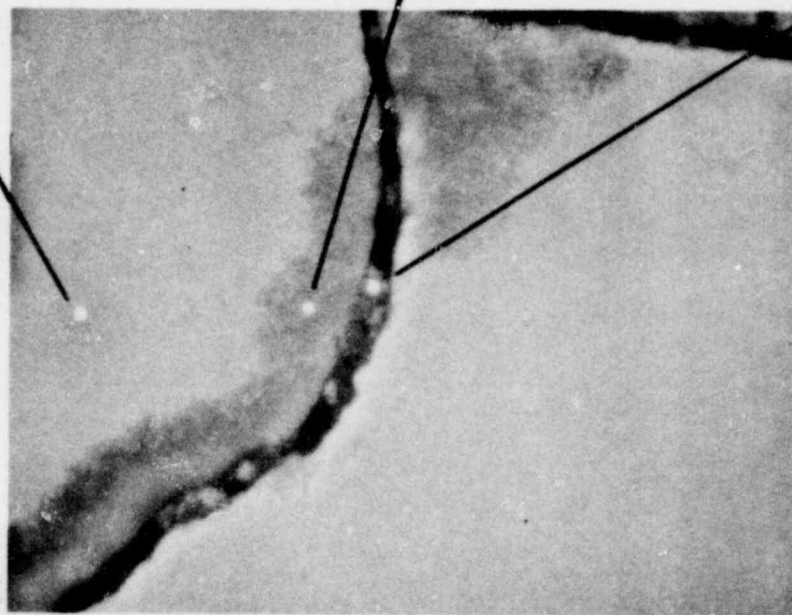
Base Metal



Cr Rich



Fe Rich

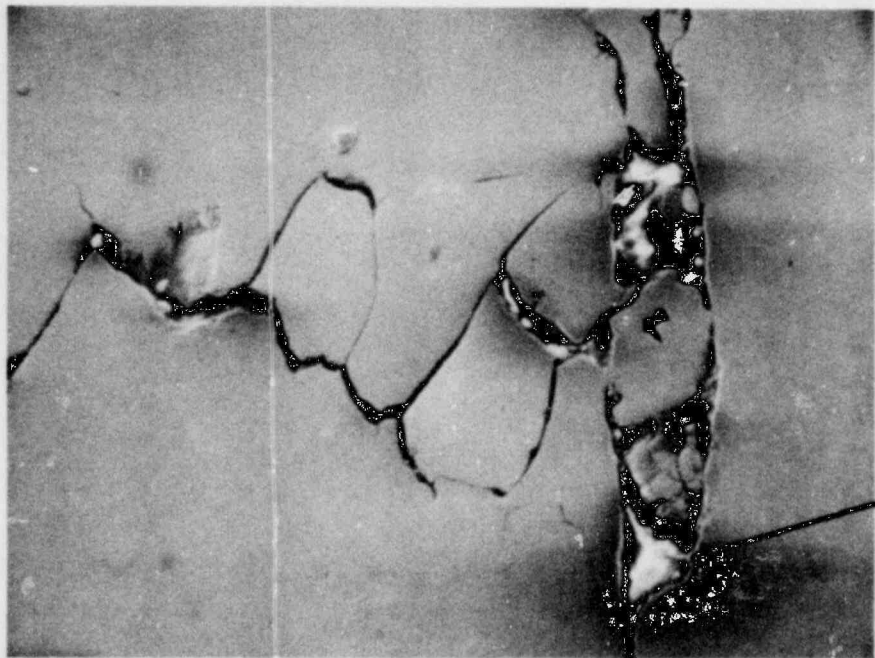


2500X

2264 233

FIGURE 17. SEM MICROGRAPH AND CORRESPONDING EDAX ANALYSES FROM SAMPLE 4
 Area shown is located within the rectangular region highlighted in Figure 6

POOR ORIGINAL



250X

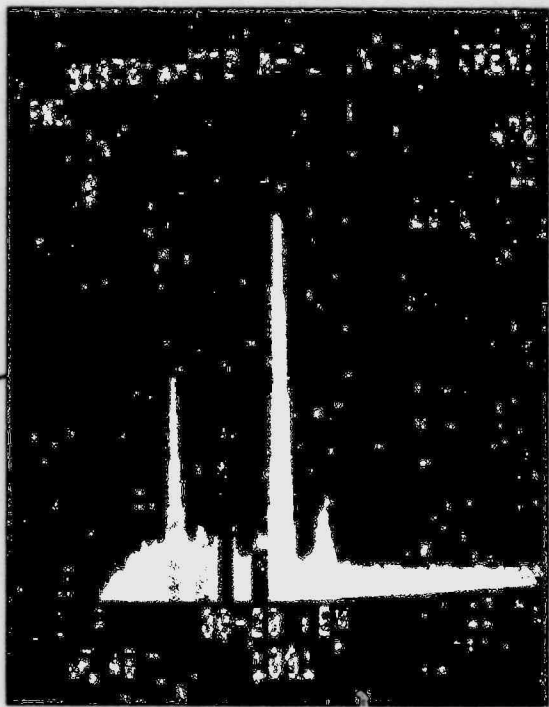
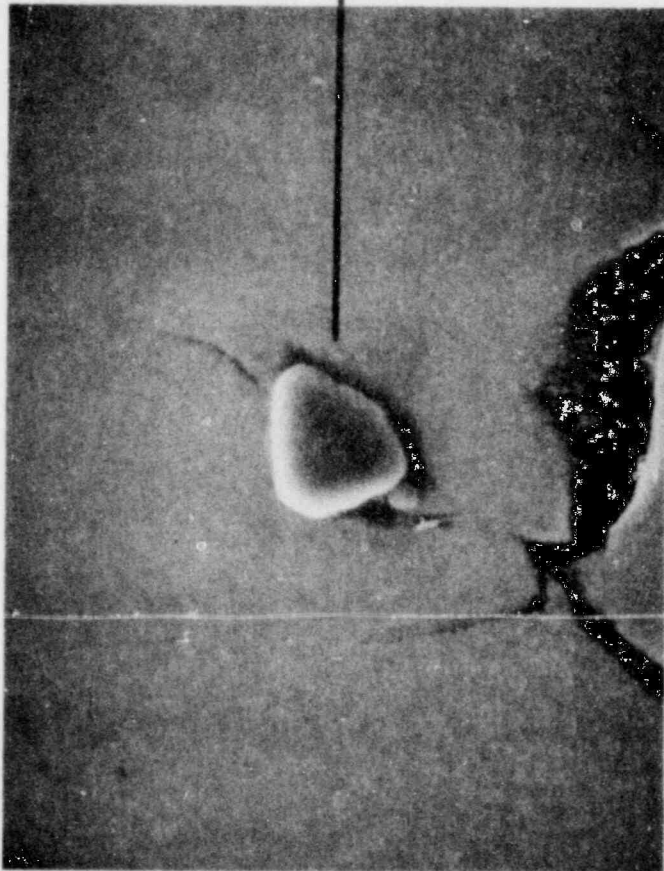
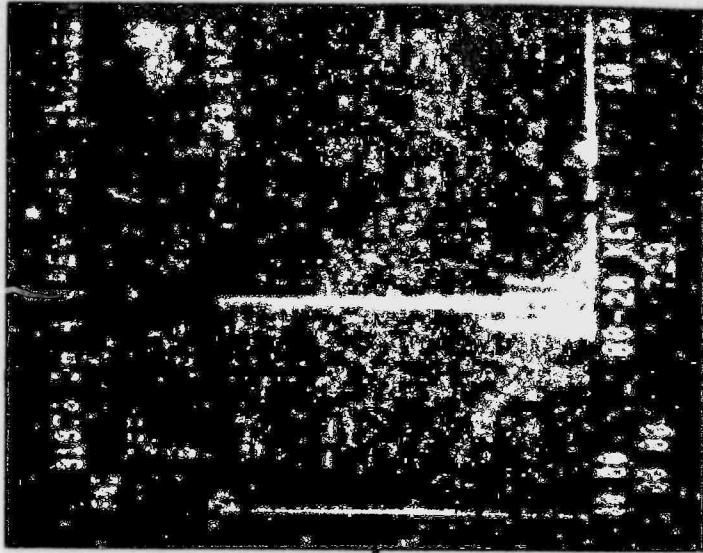


FIGURE 18. SEM MICROGRAPH AND CORRESPONDING EDAX ANALYSIS OF IRON RICH MATERIAL IN CREVICE OF SAMPLE 4

2264 234

POOR ORIGINAL

POOR ORIGINAL



1600X

FIGURE 19. SEM MICROGRAPH AND CORRESPONDING EDAX ANALYSIS OF TITANIUM INCLUSION FROM SAMPLE 4

2264 235

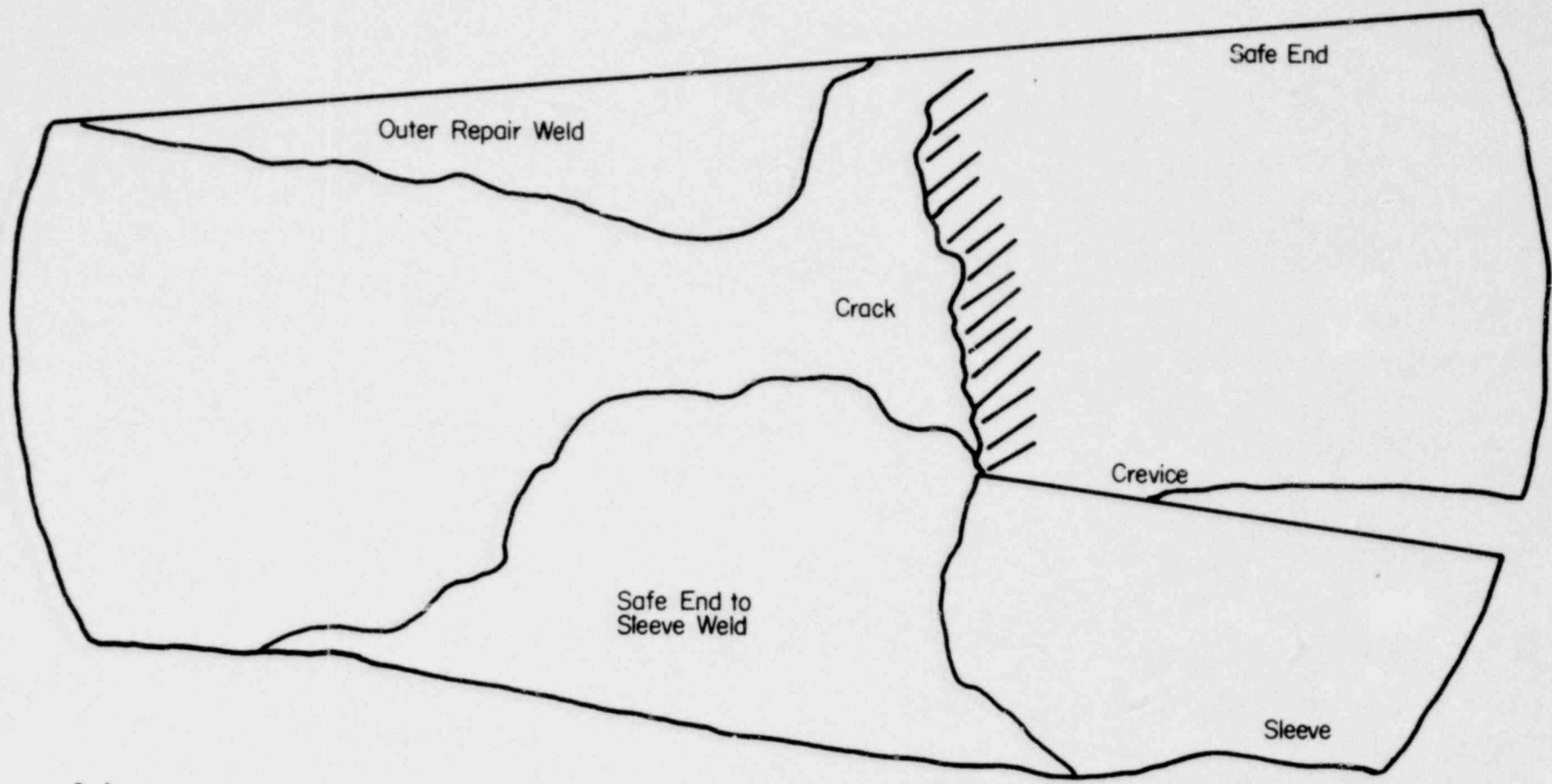


FIGURE 20. SCHEMATIC DIAGRAM OF SAFE END SAMPLE 5 INDICATING FRACTURE SURFACE EXAMINED BY SEM

2264 236

30

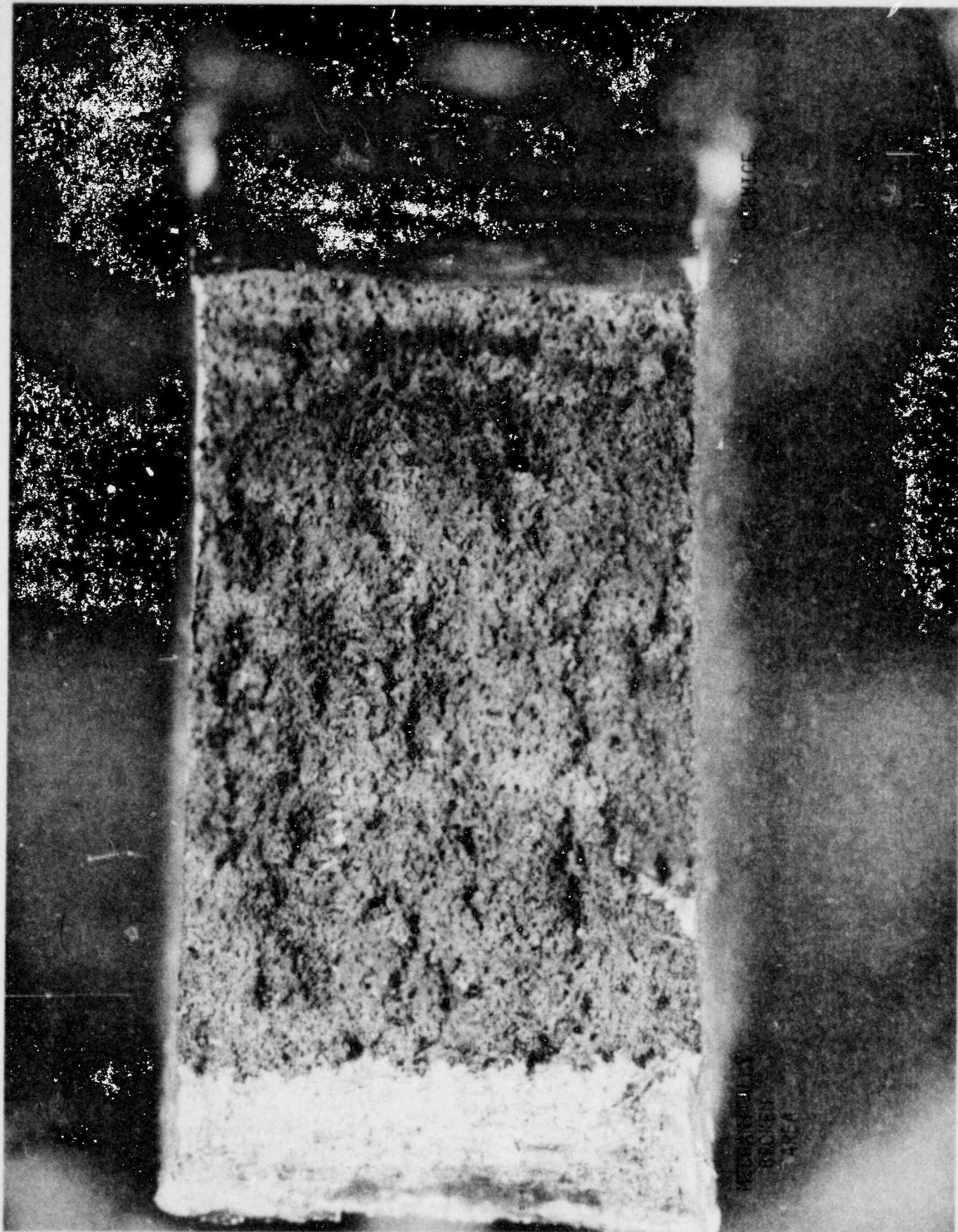
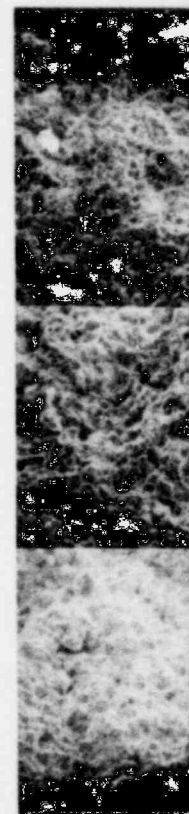
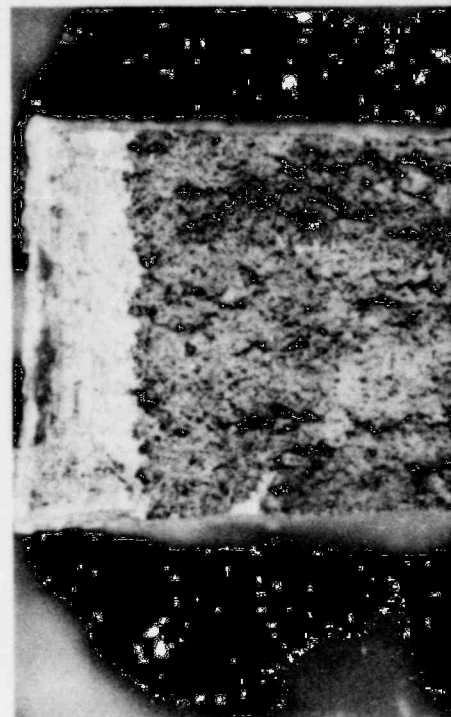


FIGURE 21. PHOTOMICROGRAPH OF FRACTURE SURFACE FROM SAMPLE 5

POOR ORIGINAL



(a) Crack Tip

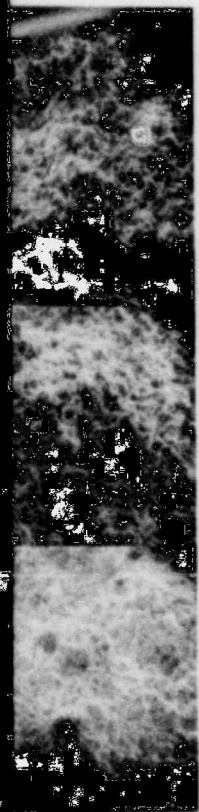
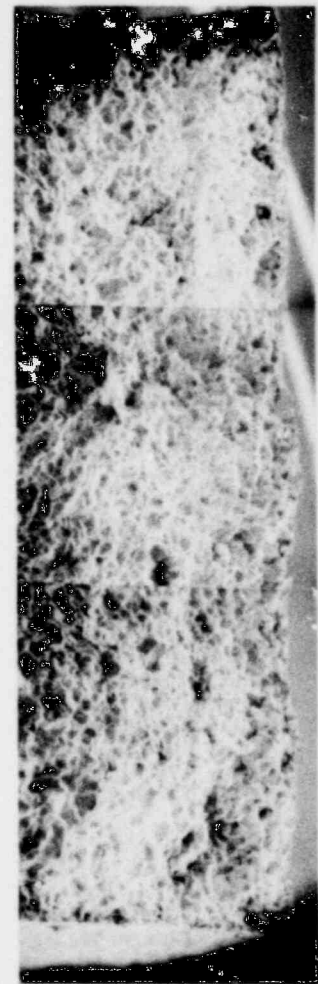
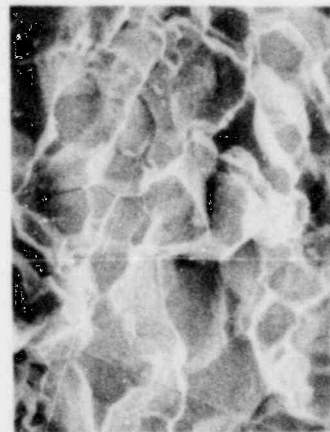
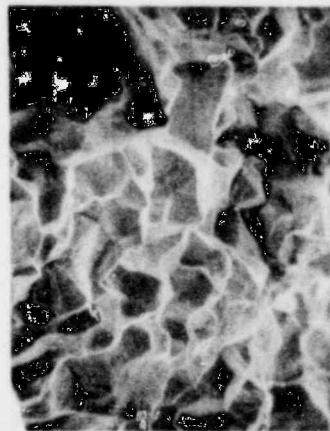
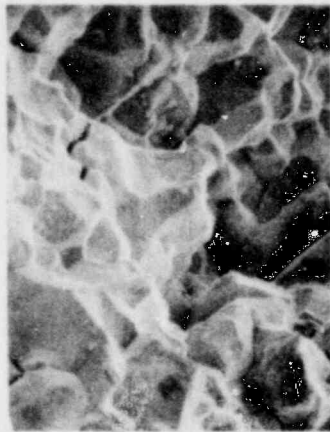


(b) Mid

FIGURE 22. SEM MICROGRAPH MONTAGES OF SAMPLE 5 FRACTURE SURFACE (a) Crack Tip, (b) Mid Fracture, (c) Near Crevice

2264 238

POOR ORIGINAL

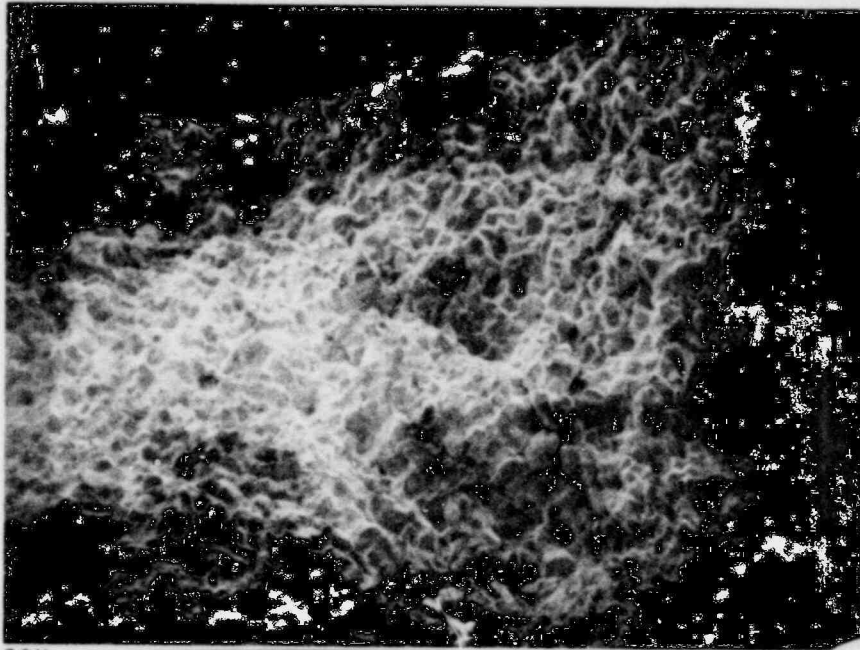


Fracture

(c) Near Crevice

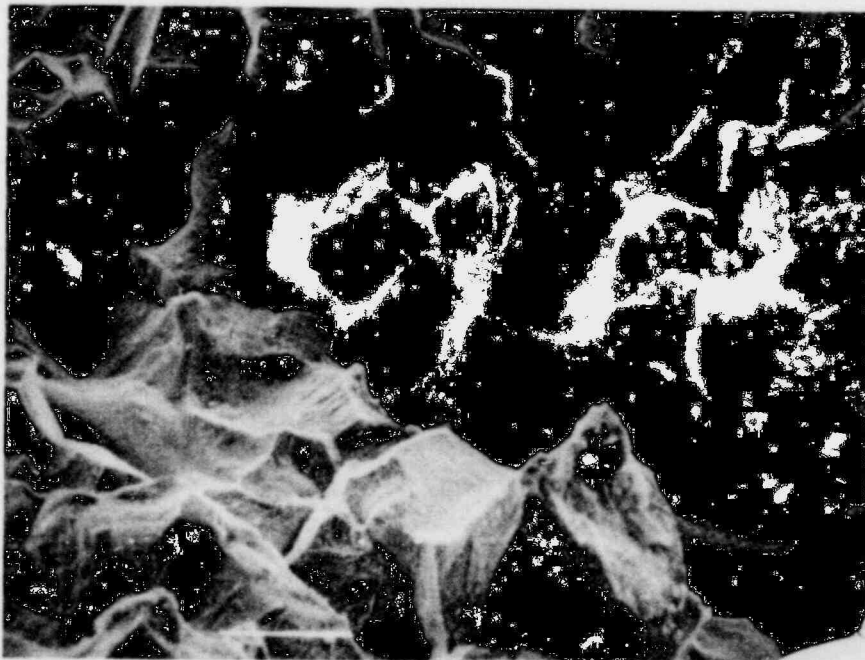
2264 239

POOR ORIGINAL



20X

(a) Typical area on fracture surface near crevice

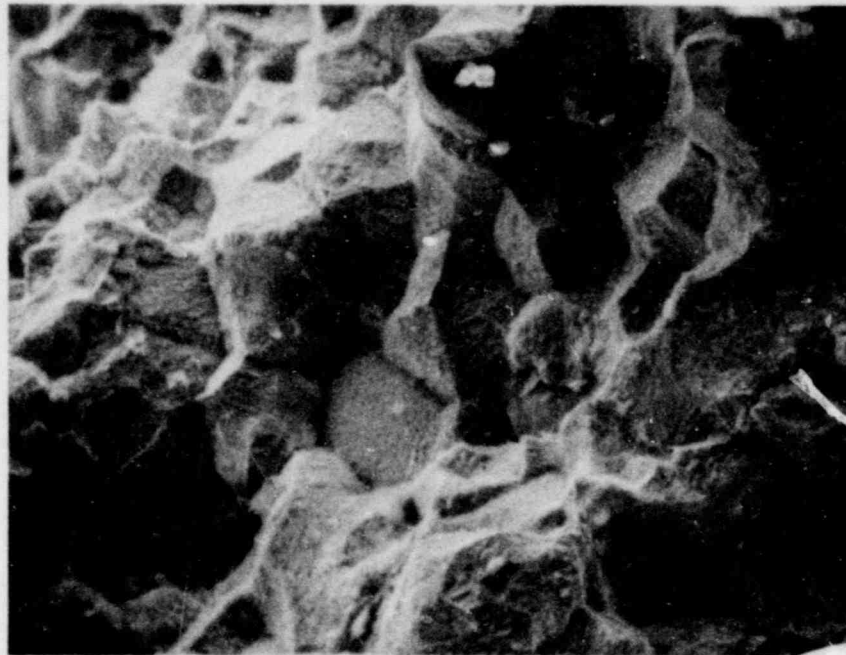


200X

(b) Actual area examined by EDAX analysis

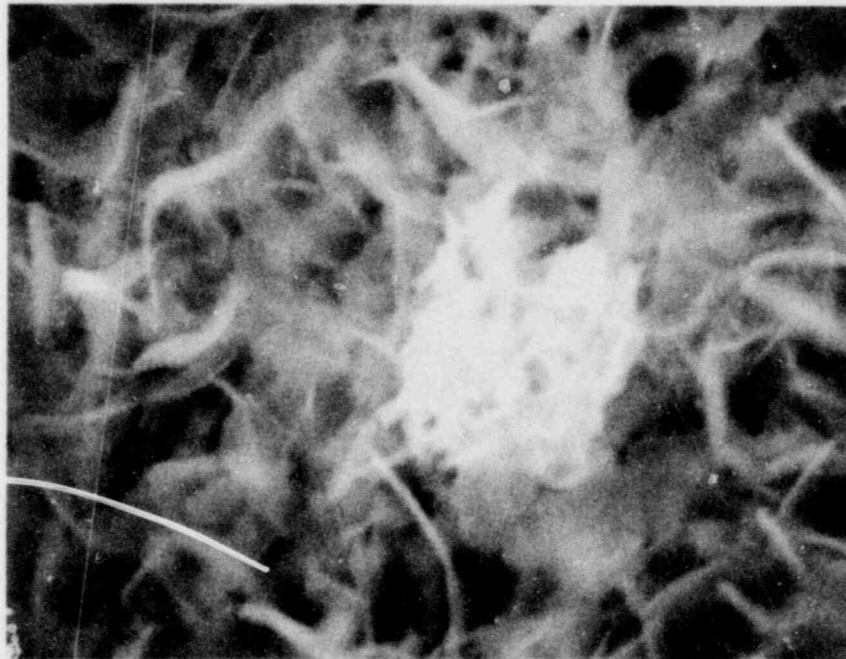
FIGURE 23. SEM FRACTOGRAPHS OF SAMPLE 5 NEAR CREVICE

2264 240



200X

(a) Actual area examined by EDAX analysis

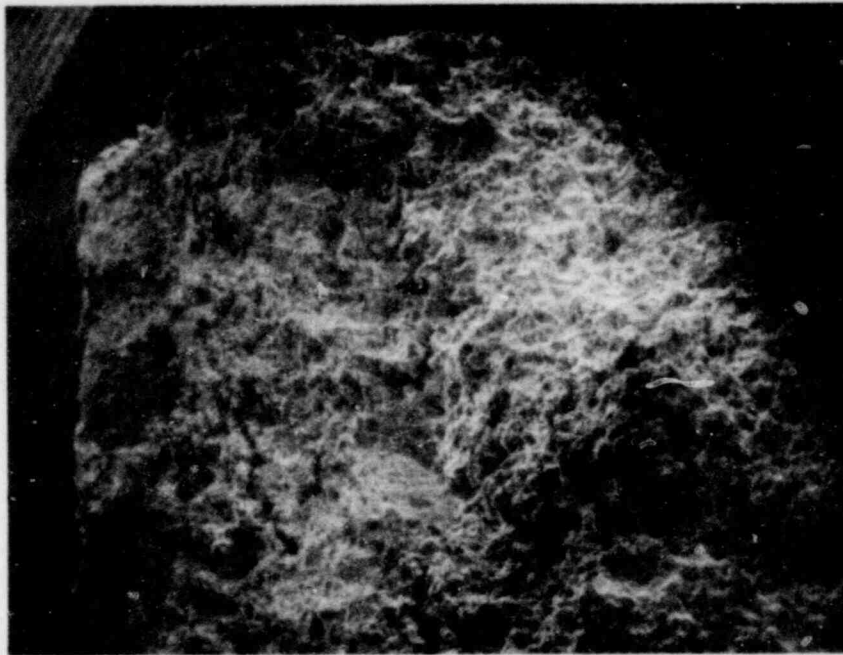


4500X

(b) Needle network of corrosion products on grain facet. Spot EDAX analysis indicated high sulfur content.

FIGURE 24. SEM FRACTOGRAPHS OF SAMPLE 5 AT MID FRACTURE

2264 241



20X

(a) Typical area on fracture surface at crack tip.



200X

(b) Actual area examined by EDAX analysis.

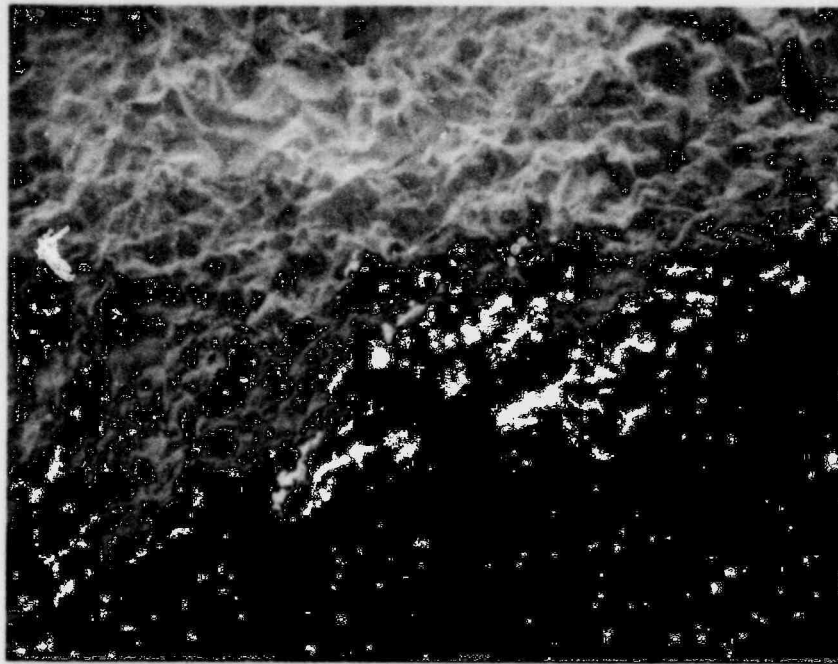
FIGURE 25. SEM FRACTOGRAPHS OF SAMPLE 5 AT CRACK TIP

2264 242

Results from EDAX analysis of Figures 23, 24, and 25 and other areas not shown indicate no significant variations from base metal composition. However, small amounts of sulfur were detected in almost all of the fracture and crevice EDAX analyses. Figure 26 presents SEM micrographs taken on the fracture surface near the crack tip. The crystalline material, magnified to 2000X in Figure 26b, was subjected to spot EDAX analysis. Results indicate high sulfur contents (-8 times greater than the highest sulfur content detected in area EDAX scans on the fracture surface). Similar crystalline structures were observed and analyzed on the crevice surface, and they too indicated relatively high sulfur content.

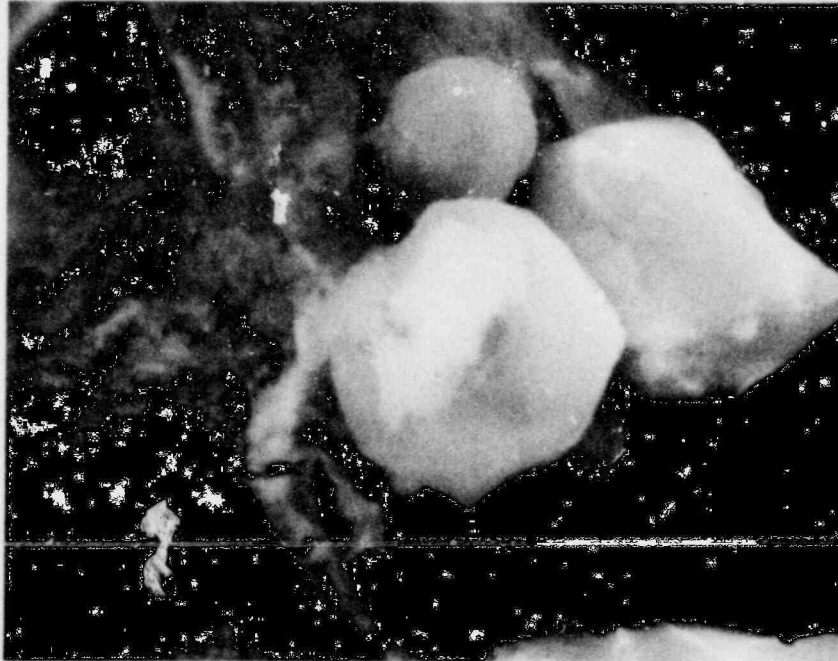
In order to characterize the sulfur distribution along a fracture surface and determine the source of the sulfur contaminants Sample 1 was mechanically fractured in the same manner as Sample 5 and examined by SEM. EDAX analyses were performed along the fracture surface at designated intervals to quantify local sulfur concentrations. A total of 11 EDAX scans were performed along a radial axis from the crevice to the tip of the crack. In addition, two EDAX analyses were performed on the mechanically broken ductile material. Each EDAX scan examined in surface area of approximately $1.6 \times 10^{-2} \text{ cm}^2$. The results of the EDAX analyses are presented as Figure 27. The relative sulfur concentration data presented in Figure 27 are plotted versus wall thickness. Based on this data an increase in relative sulfur concentration was observed with increasing crack penetration (with the exception noted directly at the crack tip). The relative sulfur concentrations measured in the ductile material beyond the crack tip indicate a significant concentration deviation from the fracture surface*. Based on the difference in relative sulfur concentrations on the fracture surface and the ductile material and the appearance of the sulfur rich particles and the high concentration of sulfur in them, it is believed that the source of sulfur in the cracks was external to the base metal material.

*It should be noted that sulfur concentration shown for the base material are intended only for comparison with those in the fracture surface. The values should not be taken as representative of actual sulfur concentration in the base metal. (See Table 3 for sulfur content in base metal.)



50X

(a) Cluster of crystalline material near crack tip.



2000X

(b) Crystalline material subject to EDAX spot analysis. Results indicate high sulfur content (>20%).

FIGURE 26. SEM FRACTOGRAPHS OF SAMPLE 5 NEAR CRACK TIP

2264 245

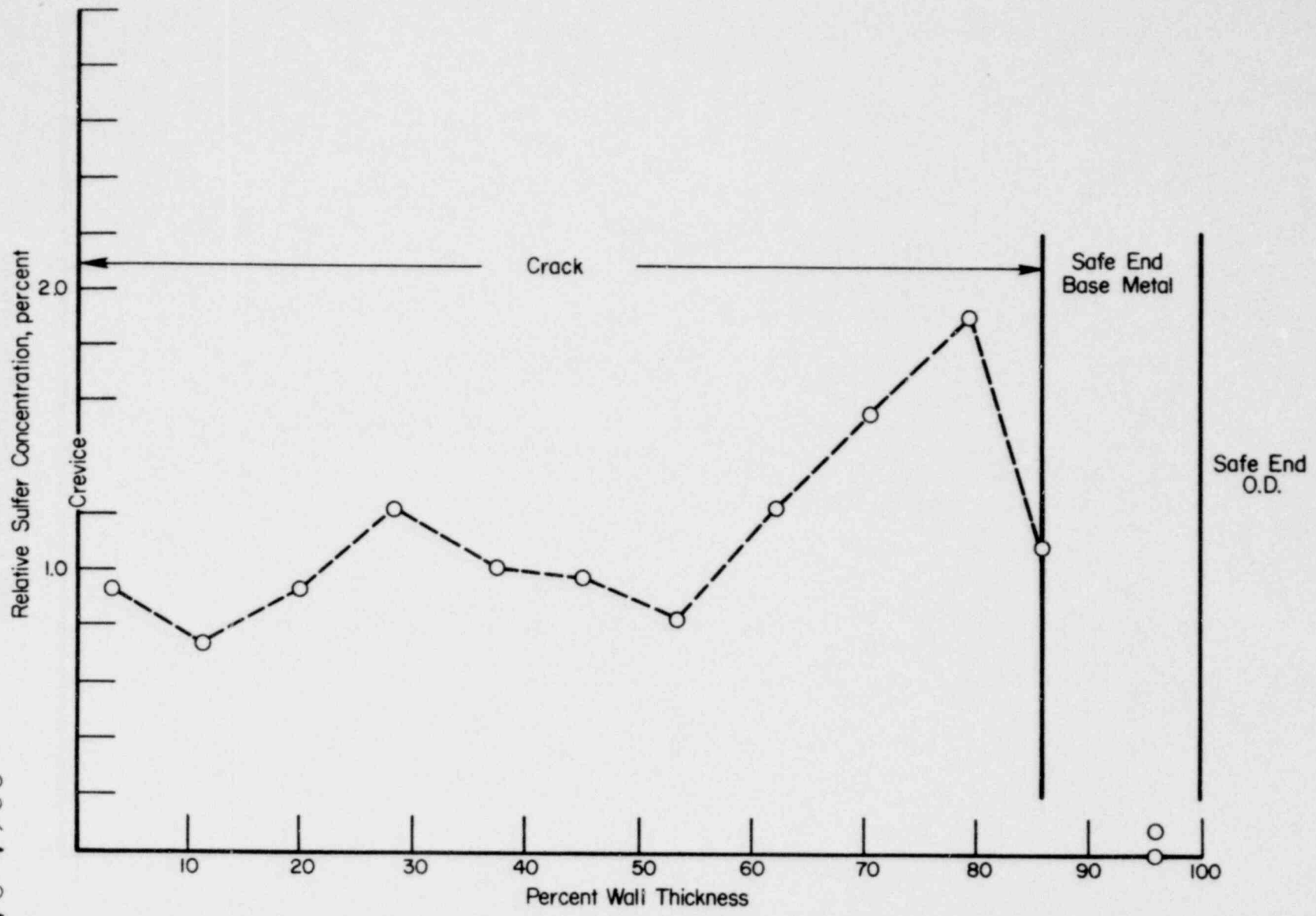


FIGURE 27. DUANE ARNOLD SAFE END SULFUR PROFILE ON FRACTURE SAMPLE No. 1

2.8 Electron Microprobe (EMP) Analysis of Duane Arnold Sample No. 2

Sample No. 2 was examined in detail with the electron microprobe. Examination consisted of 2 θ scans, X-ray mapping and area or point counting. Areas analyzed included base metal, grey phase, and weld metal. In preparation for semiquantitative analysis the sample was mounted in a stainless steel ring with epoxy, ground with SiC papers and polished with Al₂O₃ powder.

Two theta scans were obtained for each area by simultaneously scanning with LiF, PET, and KAP crystals to analyze elements from ¹¹Na through ⁹⁴Pu. In addition to the major elements Ni, Cr, and Fe, traces of Ti and Si were noted in the base metal and grey phase-crack areas. The weld metal indicated a minor amount of Mn. Results are tabulated in Table 4.

Fixed time (30 sec) area counts were then performed on the same three areas for Ni, Cr, and Fe to obtain semiquantitative analyses. The results are shown in Table 5. By comparison with pure standards, results on a first-approximation basis (e.g., no corrections for atomic number, absorption or fluorescence) were obtained. Base metal results are shown to agree reasonably well with the nominal and analytical chemistry results. Of main importance is the Cr increase in the grey phase by ~50% (relative). This analysis supports the qualitative results obtained in the scanning electron microscope (SEM).

X-ray mapping, as shown in Figure 28, compares the Ni, Cr, and Fe distribution in a grey phase-crack location. For orientation purposes the X-ray images must be compared with the electron backscatter (EBS) image, which in turn can be compared with the adjacent photomicrographs. The Ni X-ray map shows a decrease in Ni content in the Cr rich phase. The Cr image appears to indicate a slight intensity increase. Iron appears to follow the general area topography with relatively uniform distribution.

3.0 SUMMARY OF OBSERVATIONS AND CONCLUSIONS

An examination of the data presented in Section 2.0 of this report leads to the following observations and/or conclusions.

- All samples taken from the safe end and examined either by optical metallographic or SEM techniques contained part-wall cracks. No cracks were observed to penetrate the repair weld on the outer surface.

2264 246

TABLE 4. ELECTRON MICROPROBE RESULTS OF 2θ SCANS
IN BASE METAL, GREY PHASE AND WELD METAL

	<u>Base Metal</u> <u>Area 3</u>	<u>Grey Phase</u> <u>Area 1</u>	<u>Weld Metal</u> <u>Area 4</u>
<u>Elements Detected Listed in Order of Decreasing Intensity*</u>			
Major (>300 cps)	Ni Cr Fe	Ni Cr Fe	Ni Cr Fe
Minor (50-300 cps)			Mn
Trace (<50 cps)	Mg Ti Si	Mg Si Ti	Mg Ti Sr Si Nb

*Elements $_{11}\text{Na}$ through $_{92}\text{U}$.

2264 247

TABLE 5. ELECTRON MICROPROBE ANALYTICAL RESULTS FOR
Ni, Cr, Fe FROM AREA/POINT COUNTING IN BASE METAL,
GREY PHASE (POINT), AND WELD METAL*

	Base Metal	Grey Phase	Weld Metal	Inconel 600 Nominal (ASM)	Chemical Analysis (Base)
	<u>Area 3</u>	<u>Area 1</u>	<u>Area 4</u>		
Percent Ni	77	63	80	76.0	73.6
Percent Cr	15	24	17	15.5	15.6
Percent Fe	<u>7</u>	<u>9</u>	<u>5</u>	<u>8.0</u>	<u>7.8</u>
Total	99	96	102	99.5	97.0

*First approximation results do not include atomic number, absorption, or fluorescence corrections.

2264 248

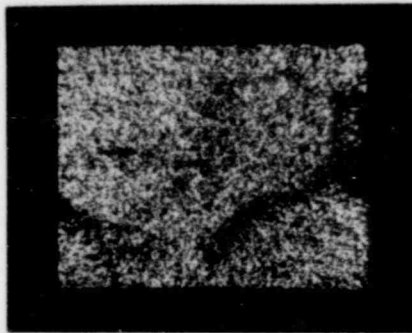
POOR ORIGINAL



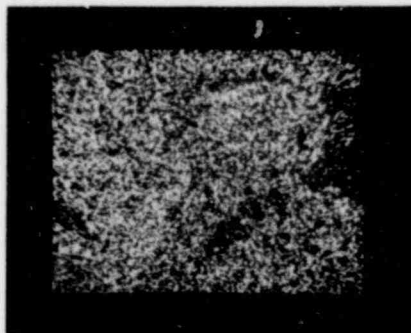
EBS
IMAGE
500X



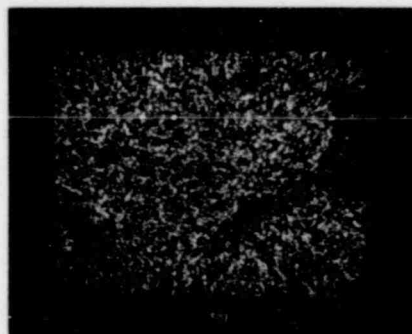
500X



Ni
X-RAY
IMAGE
500X



Cr
X-RAY
IMAGE
500X



Fe
X-RAY
IMAGE
500X

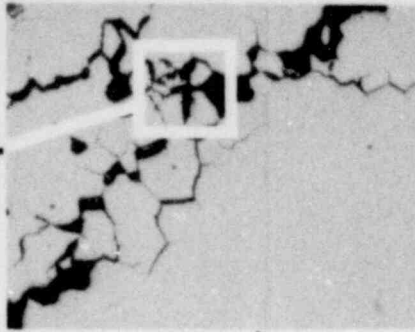
2264 249

FIGURE 28. SAMPLE #2 - MICROPROBE RESULTS

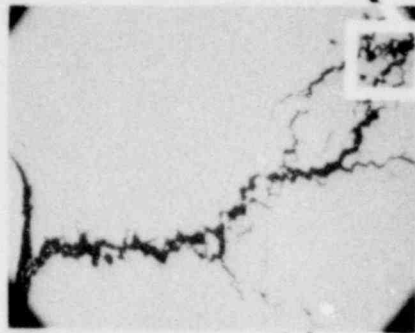
POOR ORIGINAL



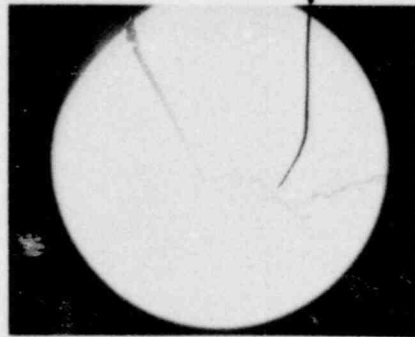
GREY PHASE



GREY
PHASE
AREA
700X



CRACK
30X



MACRO
5X

2264 250

- In all samples, the crack originated in the crevice between the sleeve and the safe end and radiated outward. No cracks were observed in the sleeve.
- The location of the cracks in all cases were in the re-solution treated region of the heat affected zone of the weld joining the safe end to the sleeve. See Figures 9 and 11.
- In the three samples examined metallographically, only one defect, namely the crack, was observed. No other crack precursors such as pitting were evident in the crevice region of any of the samples.
- All the cracks observed by metallography and fractography exhibited typical characteristics of intergranular stress corrosion cracks observed in nickel base alloys.⁽²⁻⁵⁾
- The depth of crack penetration in four of the five samples was about 80% of the safe end wall thickness. In the fifth sample which was taken from the opposite quadrant, the depth of crack was about 30%.
- From the location of the cracks, it is believed that the cause of crack initiation and subsequent propagation is not related to the repair weld on the outer surface of the safe end.
- The chemical composition of the safe end was within specification limits.
- Results of tensile tests on specimens from the safe end show no abnormalities.
- In all of the metallographic samples, small grey areas were observed around many tight branches of the cracks. These areas were found to contain relatively higher amounts of chromium. The source of the grey phase or its relationship to the cracking mechanism is not known.

2264 251

- Small amounts of sulfur were detected in almost all of the fracture surface and crevice EDAX analyses. Relatively high sulfur content was detected in a crystalline appearing material near the crack tip on the fracture surface. No sulfur was detected on the metallographically prepared samples. From the appearance of the sulfur rich particles, the amount of sulfur in these particles and the concentration profile of sulfur on the fracture surface, it is believed that the sulfur was entrapped from the environment. However, it is not known if the presence of sulfur as a contaminant contributed to the cause of cracking.

2264 252

REFERENCES

1. C. S. Tedmon, Jr., and D. A. Vermilyea, "Carbide Sensitization and Intergranular Corrosion of Nickel Base Alloys", Corrosion-Nace, 27, No. 9, pp 376-381, September (1971).
2. H. Coriou, L. Grall, P. Olivier, and H. Willermoz, "Influence of Carbon and Nickel Content on Stress Cracking of Austenitic Stainless Alloys in Pure or Chlorinated Water at 350 C", Proceedings of Conference Fundamental Aspects of Stress Corrosion Cracking, Columbus, 1967, Ohio State University, NACE (1959).
3. H. R. Copson and S. W. Dean, "Effect of Contaminant on Resistant to Stress Corrosion Cracking of Ni-Cr Alloy 600 in Pressurized Water, Corrosion, 22, pp 280-290 (1966).
4. H. A. Domian, R. H. Emanuelson, L. W. Sarver, G. J. Theus, and L. Katz, "Effect of Microstructure on Stress Corrosion Cracking of Alloy 600 in High Purity Water", Corrosion-Nace, 33, No. 1, pp 26-37, January (1977).
5. J. Blanchet, H. Corious, L. Grall, C. Mahieu, C. Otter, and G. Turluer, "Historical Review of the Principal Research Concerning the Phenomena of Cracking of Nickel Base Austenitic Alloys", Proceedings of Fifth European Congress of Corrosion, Paris, September (1973).

2264 253



Battelle

Columbus Laboratories
505 King Avenue
Columbus, Ohio 43201
Telephone (614) 424-6424

2264 254